Supplementary Information

Structure-guided development of YEATS domain inhibitors by targeting π-π-π stacking

Xin Li[1,6], Xiao-Meng Li[1,6], Yixiang Jiang[1], Zheng Liu[1], Yiwen Cui[1], Ka Yi Fung[1], Stan H. E. van der Beelen[1], Gaofei Tian[1], Liling Wan[2], Xiaobing Shi[3], C. David Allis[2], Haitao Li[4,5], Yuanyuan Li[4,5]* and Xiang David Li[1]*

[1]Department of Chemistry, The University of Hong Kong, Pokfulam Road, Hong Kong, China. [2]Laboratory of Chromatin Biology & Epigenetics, The Rockefeller University, New York, New York 10065, USA. [3]Department of Epigenetics and Molecular Carcinogenesis, The University of Texas MD Anderson Cancer Center, Houston, Texas 77030, USA. [4]MOE Key Laboratory of Protein Sciences, Beijing Advanced Innovation Center for Structural Biology, Department of Basic Medical Sciences, School of Medicine, Tsinghua University, Beijing 100084, China. [5]Tsinghua-Peking Joint Center for Life Sciences, Tsinghua University, Beijing 100084, China.

[6]These authors contributed equally to this work.

*e-mail: xiangli@hku.hk or liyuanyuan@tsinghua.edu.cn

Reagents and instruments for synthesis

Unless otherwise noted, all the chemical reagents were purchased from Sigma-Aldrich. All Fmoc- or Cbz-protected amino acids, resin for solid-phase peptide synthesis, and coupling reagents were purchased from GL Biochem. In-solution reactions were monitored by TLC silica gel 60 F254 from Merck. Flash column chromatography was performed with silica gel purchased from Grace.

^{1}H and ^{13}C NMR spectra were recorded on Bruker UltraShield 400 or 600 MHz spectrometers and were calibrated using residual undeuterated solvent as an internal reference. Chemical shifts were reported in values (ppm), and coupling constant J were reported in Hz. Peptides were analyzed by LC-MS with an Agilent 1260 Infinity HPLC system connected to a Thermo Finnigan LCQ DecaXP MS detector. Peptides were purified on a preparative HPLC system with Waters 2535 Quaternary Gradient Module, Waters 515 HPLC pump, Waters SFO System Fluidics Organizer, and Waters 2767 Sample Manager.

Synthesis of Fmoc-protected lysine derivatives.

Carboxylic acid (1.5 eq.) and NHS (1.4 eq.) were dissolved in dry THF. DCC (1.4 eq.) in dry THF was added into the above solution and stirred at r.t. overnight. The reaction mixture was filtered and to the filtrate was added Fmoc-Lys-OH·HCl (1 eq.) together with DIEA (3 eq.). The resulting reaction mixture was allowed to stir at r.t. for another 4–6 h. The pH of the mixture was adjusted to 7 with 1 M HCl. The solvent was *in vacuo*. The residue was extracted with DCM and 1 M HCl. The organic layer was washed by brine and dried over Na$_2$SO$_4$. After removal of solvent, the crude product was purified by silica gel column chromatography.


58
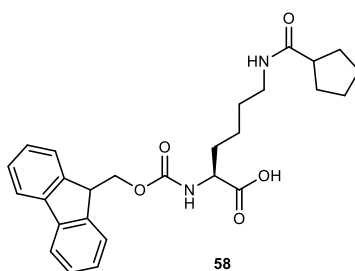
White solid, 62%. ^{1}H-NMR (DMSO-d$_6$, 400 MHz) δ 7.89 (d, 2H, J = 7.5), 7.73 (d, 3H, J = 7.2), 7.64 (d, 1H,

J = 7.96), 7.41 (t, 2H, J = 7.39), 7.33 (t, 2H, J = 7.41), 4.29–4.20 (m, 3H), 3.95–3.89 (m, 1H), 3.04 (t, 2H, J = 6.10), 1.70–1.57 (m, 8H), 1.45–1.30 (m, 6H). ^{13}C-NMR (DMSO-d$_6$, 100 MHz) δ 175.16, 174.09, 156.24, 143.88, 140.77, 127.70, 127.12, 125.35, 120.16, 65.68, 53.83, 46.72, 44.43, 38.27, 30.48, 30.04, 28.82, 25.68, 23.11. HRMS (ESI) calculated m/z for [M + Na]$^+$: 487.2203, found 487.2205.


43
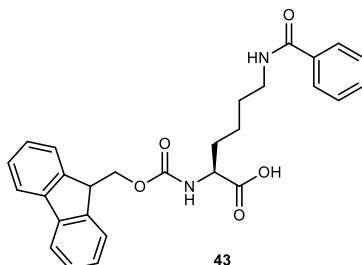
White solid, 54%. ^{1}H-NMR (DMSO-d$_6$, 400 MHz) δ 8.47 (t, 1H, J = 5.28), 7.89 (d, 2H, J = 7.48), 7.84 (d, 2H, J = 7.22), 7.72 (d, 2H, J = 7.45), 7.66 (d, 1H, J = 7.98), 7.50 (t, 1H, J = 7.20), 7.45 (d, 2H, J = 7.62), 7.40 (d, 2H, J = 7.56), 7.32 (t, 2H, J = 7.42), 4.28–4.19 (m, 3H), 3.96–3.91 (m, 1H), 3.26 (q, 2H, J = 6.47), 1.75–1.63 (m, 2H), 1.55–1.49 (m, 2H), 1.43–1.36 (m, 2H). ^{13}C-NMR (DMSO-d$_6$, 100 MHz) δ 174.07, 166.15, 156.22, 143.85, 140.75, 134.72, 131.03, 128.25, 127.68, 127.16, 127.11, 125.33, 120.15, 65.64, 53.83, 46.67, 39.01, 30.50, 28.75, 23.21. HRMS (ESI) calculated m/z for [M + Na]$^+$: 495.1890, found 495.1885.


50
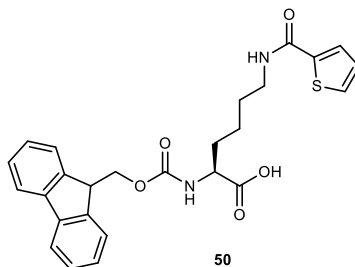
White solid, 55%. ^{1}H-NMR (DMSO-d$_6$, 400 MHz) δ 8.48 (t, 1H, J = 5.38), 7.89 (d, 2H, J = 7.48), 7.73–7.71 (m, 4H), 7.65 (d, 1H, J = 7.95), 7.41 (t, 2H, J = 7.41), 7.32 (t, 2H, J = 7.41), 7.12 (t, 1H, J = 7.56), 4.28–4.20 (m, 3H), 3.96–3.90 (m, 1H), 3.22 (q, 2H, J = 6.56), 1.76–1.61 (m, 2H), 1.55–1.45 (m, 2H), 1.42–1.35 (m, 2H). ^{13}C-NMR (DMSO-d$_6$, 100 MHz) δ 174.06, 161.02, 156.22, 143.89, 140.75, 140.30, 130.51, 127.84, 127.78, 127.68, 127.11, 125.33, 120.15, 65.63, 53.82, 46.68, 38.90, 30.49, 28.82, 23.21. HRMS (ESI) calculated m/z for [M + Na]$^+$: 501.1455, found 501.1459.

51

White solid, 61%. ^{1}H-NMR (DMSO-d$_6$, 400 MHz) δ 8.31 (t, 1H, J = 5.03), 8.10 (d, 1H, J = 1.31), 7.88 (d, 2H, J = 7.47), 7.73 (d, 2H, J = 7.44), 7.66 (d, 1H, J = 7.99), 7.55 (t, 1H, J = 4.82), 7.50 (d, 1H, J = 4.94), 7.41 (t, 2H, J = 7.40), 7.32 (t, 2H, J = 7.43), 4.29–4.20 (m, 3H), 3.95 (m, 1H), 3.23 (q, 2H, J = 6.06), 1.76–1.60 (m, 2H), 1.54–1.46 (m, 2H), 1.41–1.36 (m, 2H). ^{13}C-NMR (DMSO-d$_6$, 100 MHz) δ 174.10, 162.04, 156.25, 143.84, 140.77, 138.09, 128.40, 127.70, 127.13, 126.86, 126.62, 125.34, 120.16, 65.66, 53.86, 46.70, 38.71, 30.53, 28.85, 23.24. HRMS (ESI) calculated m/z for [M + Na]$^+$: 501.1455, found 501.1452.

54

White solid, 57%. ^{1}H-NMR (DMSO-d$_6$, 400 MHz) δ 8.64 (t, 1H, J = 5.52), 8.54 (d, 1H, J = 6.01), 7.88 (d, 2H, J = 7.50), 7.75 (s, 1H), 7.72 (d, 2H, J = 7.38), 7.66 (d, 1H, J = 7.98), 7.41 (t, 2H, J = 7.37), 7.32 (t, 2H, J = 7.41), 4.30–4.21 (m, 3H), 3.97–3.92 (m, 1H), 3.23 (q, 2H, J = 6.51), 1.75–1.57 (m, 2H), 1.54–1.44 (m, 2H), 1.38–1.35 (m, 2H). ^{13}C-NMR (DMSO-d$_6$, 100 MHz) δ 174.11, 156.45, 156.28, 153.24, 145.63, 143.87, 140.79, 128.82, 127.72, 127.14, 125.35, 120.18, 65.68, 53.85, 46.72, 38.43, 30.50, 28.67, 23.18. HRMS (ESI) calculated m/z for [M + Na]$^+$: 486.1636, found 486.1632.

47

White solid, 45%. ^{1}H-NMR (DMSO-d$_6$, 400 MHz) δ 9.93 (d, 3H, J = 4.75), 7.88 (d, 2H, J = 7.50), 7.72 (d, 2H, J = 7.42), 7.65 (t, 2H, J = 4.46), 7.40 (t, 2H, J = 7.40), 7.31 (t, 2H, J = 7.40), 4.31–4.19 (m, 3H), 3.96–3.91

(m, 1H), 3.29 (q, 2H, $J = 6.62$), 1.77–1.63 (m, 2H), 1.59–1.50 (m, 2H), 1.44–1.35 (m, 2H). ^{13}C-NMR (DMSO-d$_6$, 100 MHz) δ 174.09, 162.43, 158.28, 157.66, 156.23, 143.88, 140.76, 127.69, 127.12, 125.34, 122.91, 120.16, 65.64, 53.91, 46.70, 38.94, 30.55, 28.70, 23.20. HRMS (ESI) calculated m/z for [M + Na]$^+$: 497.1795, found 497.1790.

45
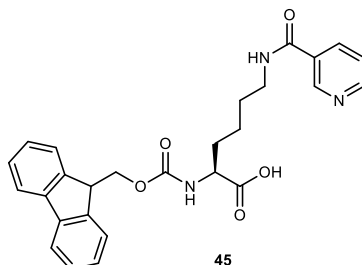
White solid, 43%. ^{1}H-NMR (DMSO-d$_6$, 400 MHz) δ 9.03 (s, 1H), 8.70 (t, 2H, $J = 5.26$), 8.24 (d, 1H, $J = 7.97$), 7.89 (d, 2H, $J = 7.49$), 7.72 (d, 2H, $J = 7.44$), 7.63 (d, 1H, $J = 7.99$), 7.56–7.53 (m, 1H), 7.41 (t, 2H, $J = 7.40$), 7.31 (t, 2H, $J = 7.40$), 4.28–4.19 (m, 3H), 3.97–3.91 (m, 1H), 3.28 (q, 2H, $J = 6.71$), 1.77–1.61 (m, 2H), 1.59–1.50 (m, 2H), 1.47–1.37 (m, 2H). ^{13}C-NMR (DMSO-d$_6$, 100 MHz) δ 174.00, 164.46, 156.21, 151.01, 147.73, 143.87, 140.75, 135.73, 130.43, 127.68, 127.10, 125.32, 123.78, 120.14, 65.64, 53.79, 46.68, 38.92, 30.48, 28.58, 23.16. HRMS (ESI) calculated m/z for [M + Na]$^+$: 496.1843, found 496.1842.


44
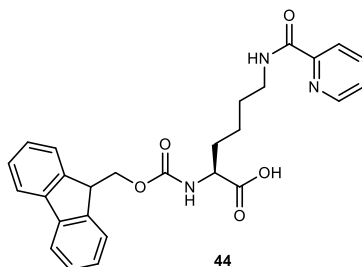
White solid, 52%. ^{1}H-NMR (DMSO-d$_6$, 400 MHz) δ 8.82 (t, 1H, $J = 5.96$), 8.61 (d, 1H, $J = 4.69$), 8.04 (d, 1H, $J = 7.69$), 7.97 (td, 1H, $J = 7.57, 1.49$), 7.88 (d, 2H, $J = 7.48$), 7.72 (d, 2H, $J = 7.46$), 7.66 (d, 1H, $J = 7.96$), 7.58–7.55 (m, 1H), 7.40 (t, 2H, $J = 7.44$), 7.31 (t, 2H, $J = 7.44$), 4.28–4.19 (m, 3H), 3.97–3.91 (m, 1H), 3.31 (q, 2H, $J = 6.79$), 1.77–1.61 (m, 2H), 1.60–1.49 (m, 2H), 1.42–1.34 (m, 2H). ^{13}C-NMR (DMSO-d$_6$, 100 MHz) δ 174.04, 163.79, 156.21, 150.16, 148.38, 143.84, 140.75, 137.80, 127.69, 127.12, 126.44, 125.33, 121.86, 120.16, 65.63, 53.86, 46.68, 38.62, 30.50, 28.86, 23.19. HRMS (ESI) calculated m/z for [M + Na]$^+$: 496.1843, found 496.1845.

49
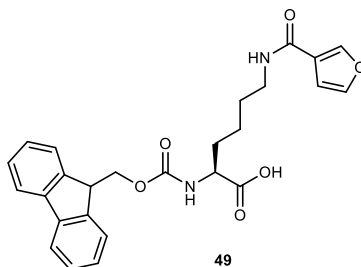
White solid, 70%. ^{1}H-NMR (DMSO-d$_6$, 400 MHz) δ 8.19–8.14 (m, 2H), 7.89 (d, 2H, J = 7.48), 7.73–7.69 (m, 3H), 7.65 (d, 1H, J = 7.98), 7.41 (t, 2H, J = 7.38), 7.32 (t, 2H, J = 7.43), 6.84 (d, 2H, J = 1.28), 4.29–4.20 (m, 3H), 3.96–3.91 (m, 1H), 3.20 (q, 2H, J = 6.29), 1.76–1.59 (m, 2H), 1.53–1.45 (m, 2H), 1.41–1.34 (m, 2H). ^{13}C-NMR (DMSO-d$_6$, 100 MHz) δ 174.09, 161.55, 156.25, 144.96, 143.95, 143.85, 140.77, 127.69, 127.12, 125.34, 123.00, 120.17, 109.00, 65.66, 53.85, 46.70, 38.44, 30.52, 28.86, 23.24. HRMS (ESI) calculated m/z for [M + Na]$^+$: 485.1683, found 485.1684.

46
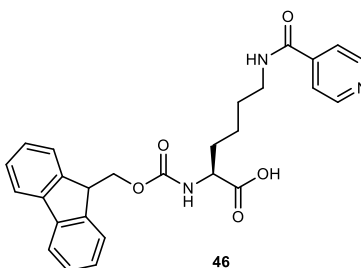
White solid, 48%. ^{1}H-NMR (DMSO-d$_6$, 400 MHz) δ 8.77 (t, 1H, J = 5.38), 8.71 (d, 2H, J = 5.36), 7.89 (d, 2H, J = 7.52), 7.75 (d, 2H, J = 5.67), 7.72 (d, 2H, J = 7.39), 7.65 (d, 1H, J = 8.04), 7.41 (t, 2H, J = 7.34), 7.31 (t, 2H, J = 7.46), 4.27–4.19 (m, 3H), 3.95–3.90 (m, 1H), 3.27 (q, 2H, J = 6.04), 1.72–1.62 (m, 2H), 1.55–1.49 (m, 2H), 1.39–1.35 (m, 2H). ^{13}C-NMR (DMSO-d$_6$, 100 MHz) δ 174.09, 164.44, 156.23, 149.68, 143.85, 142.16, 140.78, 127.70, 127.12, 125.34, 121.58, 120.17, 65.66, 53.83, 46.71, 39.18, 30.50, 28.52, 23.20. HRMS (ESI) calculated m/z for [M + Na]$^+$: 496.1843, found 496.1842.

52
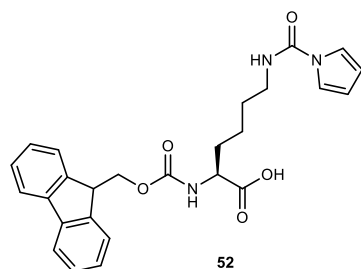
White solid, 62%. ^{1}H-NMR (DMSO-d$_6$, 400 MHz) δ 8.16 (t, 1H, J = 5.35), 7.89 (d, 2H, J = 7.49), 7.72 (d, 2H, J = 7.43), 7.63 (d, 1H, J = 7.96), 7.41 (t, 2H, J = 7.41), 7.37 (t, 2H, J = 1.93), 7.32 (t, 2H, J = 7.42), 6.19

(t, 2H, J = 2.20), 4.29–4.20 (m, 3H), 3.96–3.91 (m, 1H), 3.21 (q, 2H, J = 6.04), 1.78–1.59 (m, 2H), 1.56–1.46

(m, 2H), 1.43–1.35 (m, 2H). ^{13}C-NMR (DMSO-d$_6$, 100 MHz) δ 173.98, 156.19, 150.44, 143.86, 140.73,

127.65, 127.07, 125.29, 120.12, 118.60, 110.80, 65.62, 53.79, 46.68, 39.88, 30.46, 28.69, 23.05. HRMS (ESI)

calculated m/z for [M + Na]$^+$: 484.1843, found 484.1840.

57
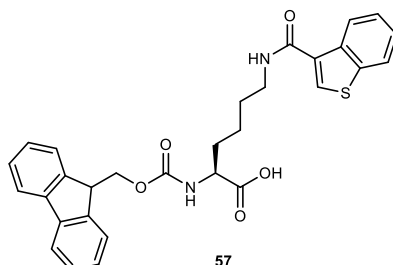
White solid, 59%. ^{1}H-NMR (DMSO-d$_6$, 400 MHz) δ 8.77 (t, 1H, J = 5.38), 8.07 (s, 1H), 8.00 (d, 1H, J = 6.96),

7.91 (d, 1H, J = 8.32), 7.87 (d, 2H, J = 7.43), 7.71 (d, 2H, J = 7.42), 7.67 (d, 1H, J = 8.00), 7.46–7.37 (m, 4H),

7.30 (t, 2H, J = 7.38), 4.28–4.19 (m, 3H), 3.98–3.93 (m, 1H), 3.28 (q, 2H, J = 6.14), 1.79–1.60 (m, 2H),

1.56–1.45 (m, 2H), 1.43–1.38 (m, 2H). ^{13}C-NMR (DMSO-d$_6$, 100 MHz) δ 174.09, 161.44, 156.25, 143.88,

140.75, 140.32, 140.17, 139.25, 127.68, 127.11, 126.13, 125.34, 125.13, 124.92, 124.49, 122.82, 120.16,

65.65, 53.83, 46.69, 39.18, 30.53, 28.71, 23.26. HRMS (ESI) calculated m/z for [M + Na]$^+$: 551.1611, found

551.1607.

55
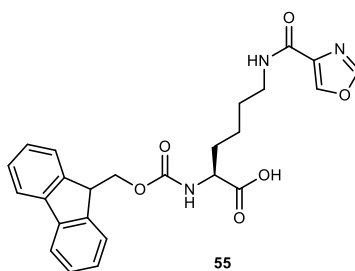
White solid, 53%. ^{1}H-NMR (DMSO-d$_6$, 400 MHz) δ 8.58 (s, 1H), 8.49 (s, 1H), 8.33 (t, 1H, J = 5.51), 7.89 (d,

2H, J = 7.48), 7.72 (d, 2H, J = 7.43), 7.64 (d, 1H, J = 7.95), 7.41 (t, 2H, J = 7.37), 7.30 (t, 2H, J = 7.42),

4.28–4.20 (m, 3H), 3.91 (m, 1H), 3.21 (q, 2H, J = 6.36), 1.73–1.61 (m, 2H), 1.50–1.47 (m, 2H), 1.37–1.33

(m, 2H). ^{13}C-NMR (DMSO-d$_6$, 100 MHz) δ 174.07, 159.82, 156.23, 152.22, 143.88, 141.69, 140.76, 135.82,

127.70, 127.12, 125.35, 120.17, 65.64, 53.89, 46.70, 39.20, 30.50, 28.83, 23.15. HRMS (ESI) calculated m/z

for [M + Na]$^+$: 486.1636, found 486.1638.

48
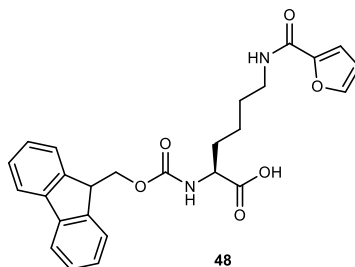
White solid, 74%. ^{1}H-NMR (DMSO-d$_6$, 400 MHz) δ 8.37 (t, 1H, J = 5.41), 7.89 (d, 2H, J = 7.48), 7.79 (s, 1H), 7.72 (d, 2H, J = 7.44), 7.65 (d, 1H, J = 7.90), 7.41 (t, 2H, J = 7.39), 7.32 (t, 2H, J = 7.42), 7.06 (d, 1H, J = 3.29), 6.60 (d, 1H, J = 1.43), 4.29–4.20 (m, 3H), 3.95–3.89 (m, 1H), 3.20 (q, 2H, J = 6.29), 1.73–1.58 (m, 2H), 1.52–1.42 (m, 2H), 1.38–1.32 (m, 2H). ^{13}C-NMR (DMSO-d$_6$, 100 MHz) δ 174.07, 157.75, 156.23, 148.14, 144.80, 143.84, 140.77, 127.70, 127.12, 125.35, 120.17, 113.11, 111.82, 65.65, 53.85, 46.70, 38.26, 30.49, 28.84, 23.18. HRMS (ESI) calculated m/z for [M + Na]$^+$: 485.1683, found 485.1681.

56
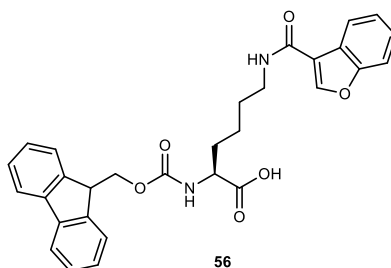
White solid, 72%. ^{1}H-NMR (DMSO-d$_6$, 400 MHz) δ 8.75 (t, 1H, J = 5.28), 7.87 (d, 2H, J = 7.48), 7.75 (d, 1H, J = 7.74), 7.71 (d, 2H, J = 7.41), 7.64 (t, 2H, J = 8.67), 7.51 (s, 1H), 7.45 (t, 1H, J = 7.66), 7.39 (t, 2H, J = 7.41), 7.34–7.28 (m, 3H) 4.28–4.19 (m, 3H), 3.93 (m, 1H), 3.27 (q, 2H, J = 6.22), 1.75–1.58 (m, 2H), 1.55–1.50 (m, 2H), 1.41–1.36 (m, 2H). ^{13}C-NMR (DMSO-d$_6$, 100 MHz) δ 174.07, 158.07, 156.23, 154.21, 149.40, 143.88, 140.75, 127.67, 127.24, 127.10, 126.74, 125.32, 123.70, 122.74, 120.15, 111.80, 109.20, 65.63, 53.84, 46.68, 38.56, 30.50, 28.72, 23.20. HRMS (ESI) calculated m/z for [M + Na]$^+$: 535.1840, found 535.1837.

53
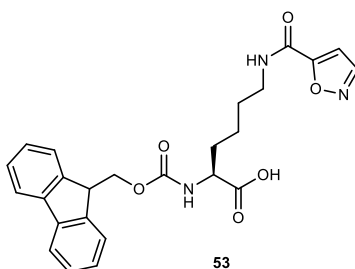
White solid, 50%. ^{1}H-NMR (DMSO-d$_6$, 400 MHz) δ 8.95 (t, 1H, J = 5.40), 8.71 (d, 1H, J = 1.67), 7.88 (d,

2H, $J = 7.49$), 7.72 (d, 2H, $J = 7.19$), 7.63 (d, 1H, $J = 7.93$), 7.41 (t, 2H, $J = 7.38$), 7.32 (t, 2H, $J = 7.40$), 7.02 (d, 1H, $J = 1.67$), 4.29–4.20 (m, 3H), 3.96–3.91 (m, 1H), 3.25 (q, 2H, $J = 6.36$), 1.75–1.59 (m, 2H), 1.55–1.43 (m, 2H), 1.38–1.35 (m, 2H). ^{13}C-NMR (DMSO-d$_6$, 100 MHz) δ 174.00, 162.98, 156.21, 155.51, 151.66, 143.83, 140.75, 127.67, 127.10, 125.31, 120.14, 105.72, 65.62, 53.81, 46.70, 38.66, 30.44, 28.41, 23.11. HRMS (ESI) calculated m/z for $[M + Na]^+$: 486.1636, found 486.1638.
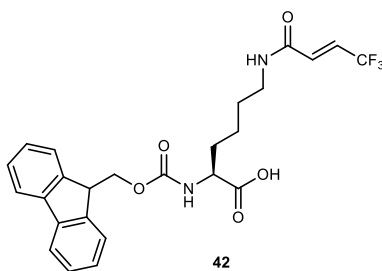
White solid, 37%. ^{1}H-NMR (DMSO-d$_6$, 400 MHz) δ 8.54 (s, 1H), 7.89 (d, 2H, $J = 7.38$), 7.72 (d, 2H, $J = 6.72$), 7.61 (d, 1H, $J = 7.74$), 7.41 (t, 2H, $J = 7.22$), 7.32 (t, 2H, $J = 7.31$), 6.75 (s, 2H), 4.29–4.22 (m, 3H), 3.92–3.91 (m, 1H), 3.16 (q, 2H, $J = 5.90$), 1.71–1.60 (m, 2H), 1.50–1.44 (m, 2H), 1.36–1.34 (m, 2H). ^{13}C-NMR (DMSO-d$_6$, 100 MHz) δ 173.97, 161.74, 156.19, 143.82, 140.74, 133.04, 127.66, 127.08, 125.52, 125.30, 125.18, 120.13, 65.62, 53.79, 46.70, 38.75, 30.44, 28.37, 23.13. ^{19}F-NMR (DMSO-d$_6$, 376 MHz) δ -63.24. HRMS (ESI) calculated m/z for $[M + Na]^+$: 513.1608, found 513.1611.

Peptide synthesis and purification.

Peptides were synthesized on either Rink-Amide MBHA resin followed standard Fmoc-based solid-phase peptide synthesis protocol. After the coupling of all amino acids, the removal of protecting groups and cleavage of peptides from the resin were done by incubating the resin with cleavage cocktail containing 95% TFA, 2.5% TIS, 1.5% H$_2$O and, 1% thioanisole for 2 h. Peptides were purified by preparative HPLC with an XBridge Prep OBDTM C18 column (30 mm × 250 mm, 10 μm, Waters). Mobile phase used were water with 0.1% TFA (buffer A) and 90% ACN in water with 0.1% TFA (buffer B). The purity (> 95%) and identity of peptides were confirmed by LC-MS.
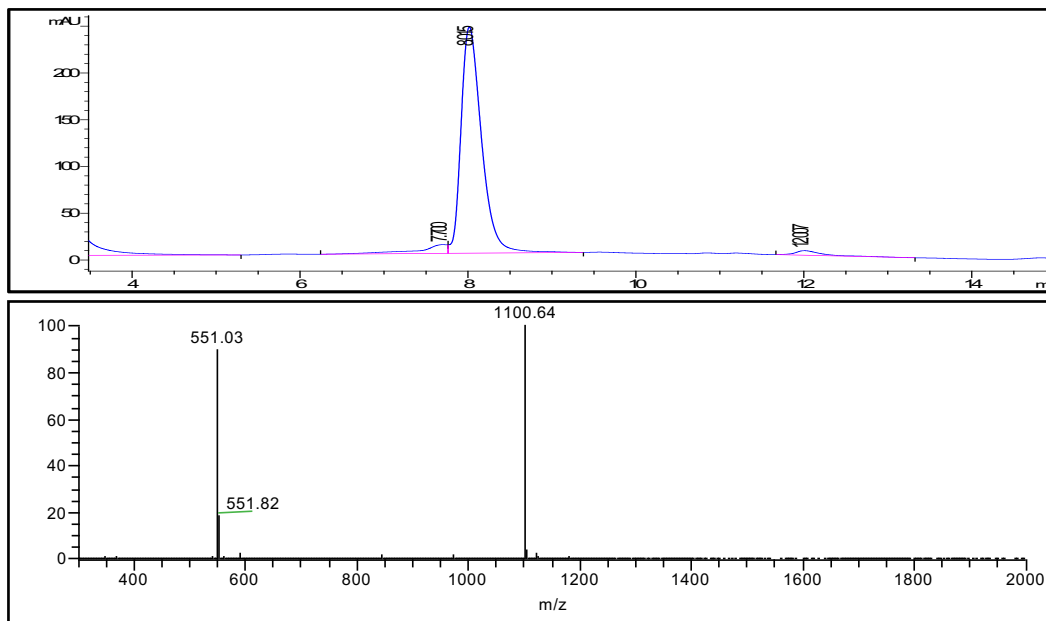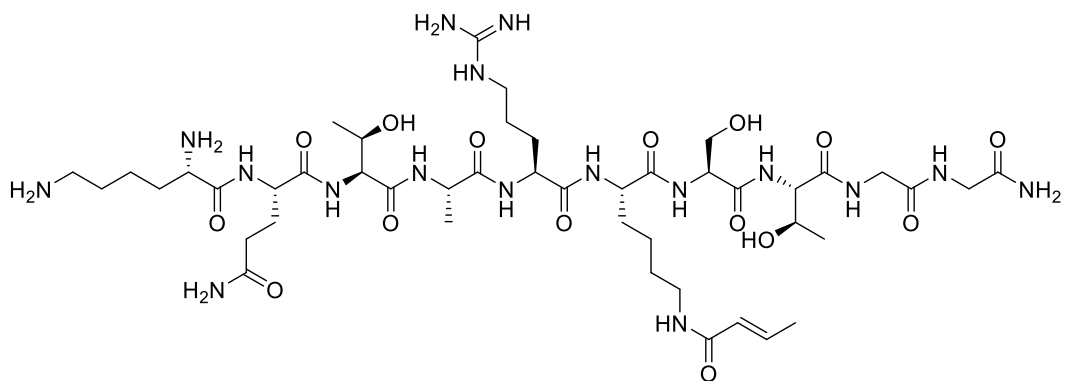
LC−MS analysis of peptide H3K9cr: KQTARKcrSTGG.

Calculated m/z for $[M + H]^+$: 1100.62, found: 1100.64; calculated m/z for $[M + 2H]^{2+}$: 550.81, found: 551.03.
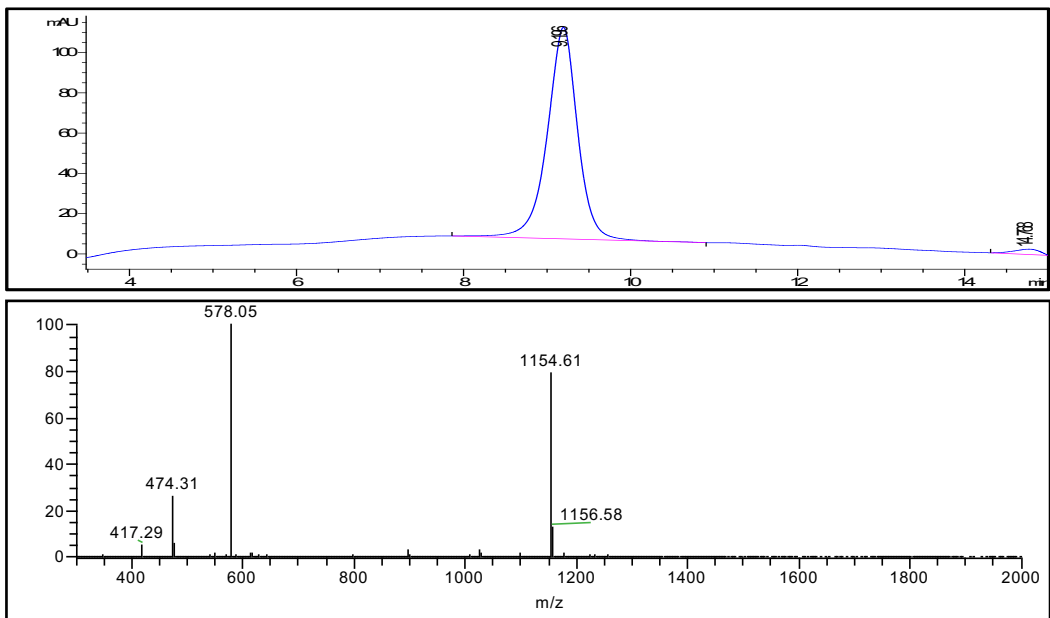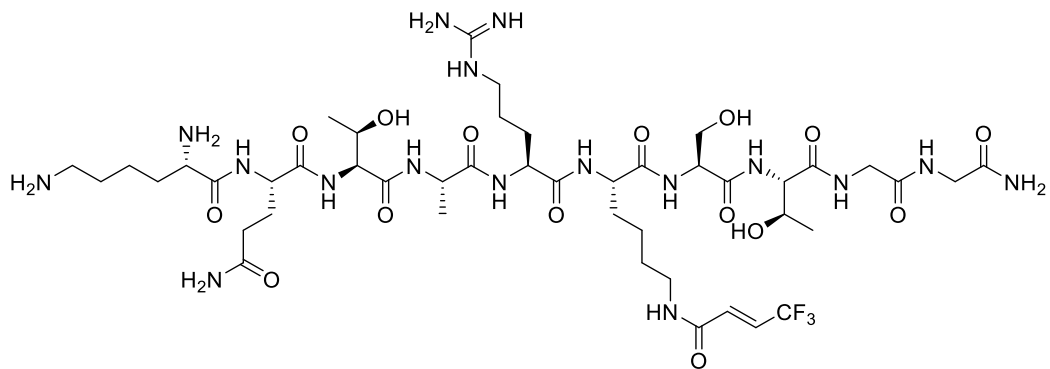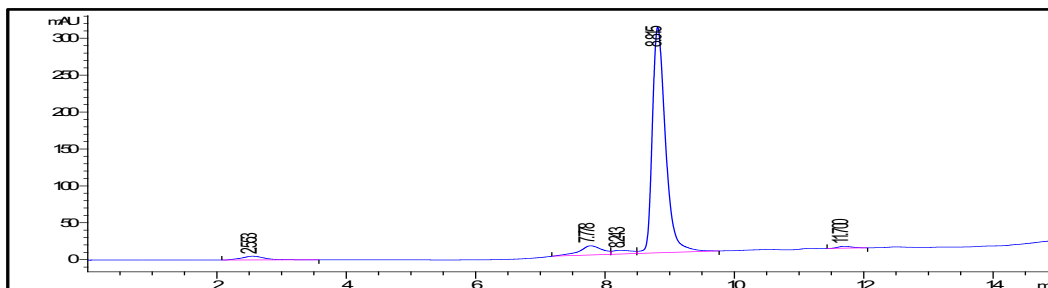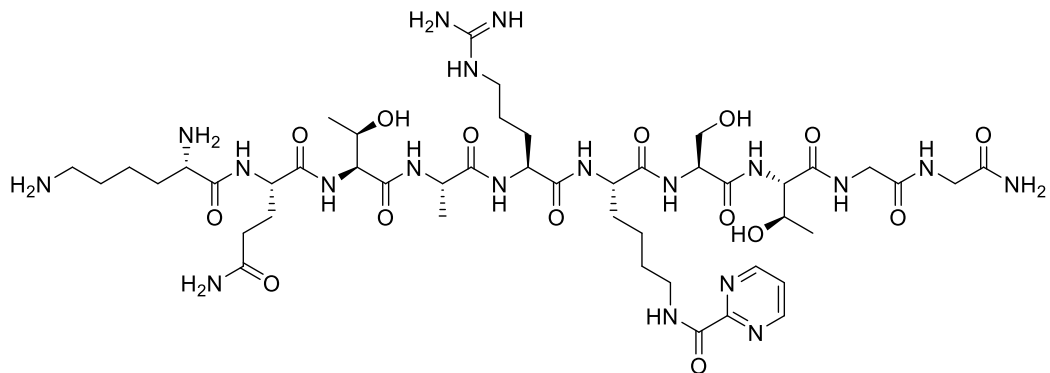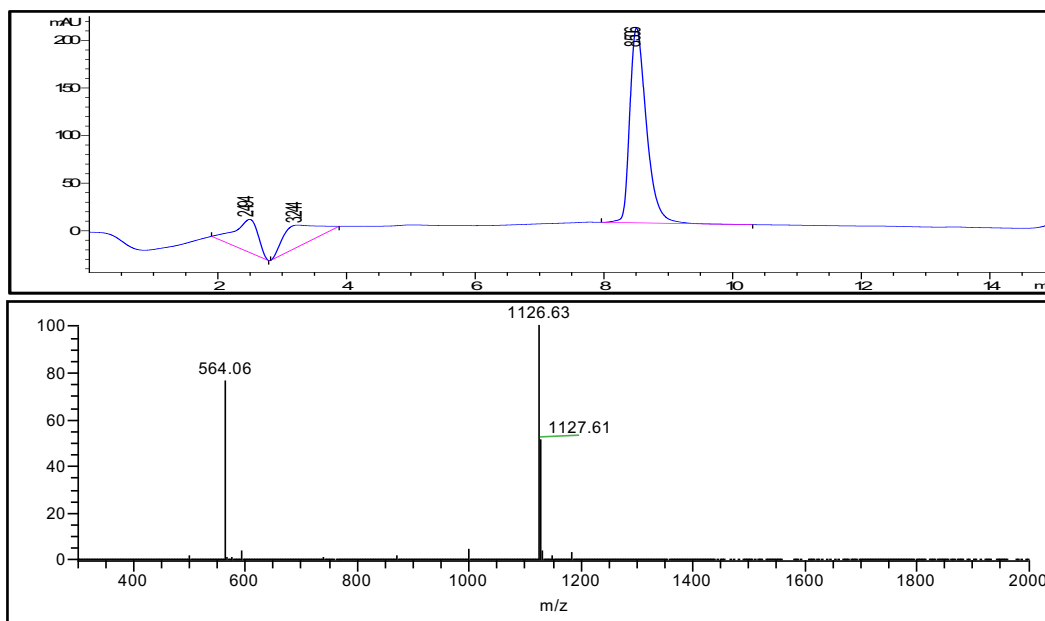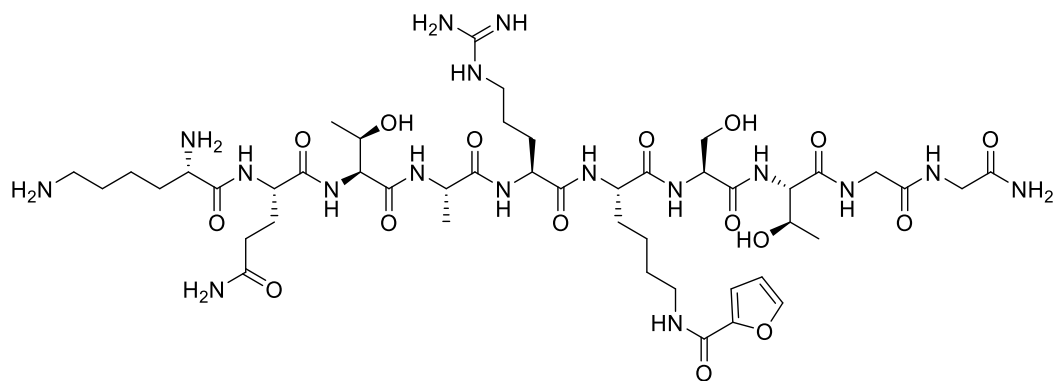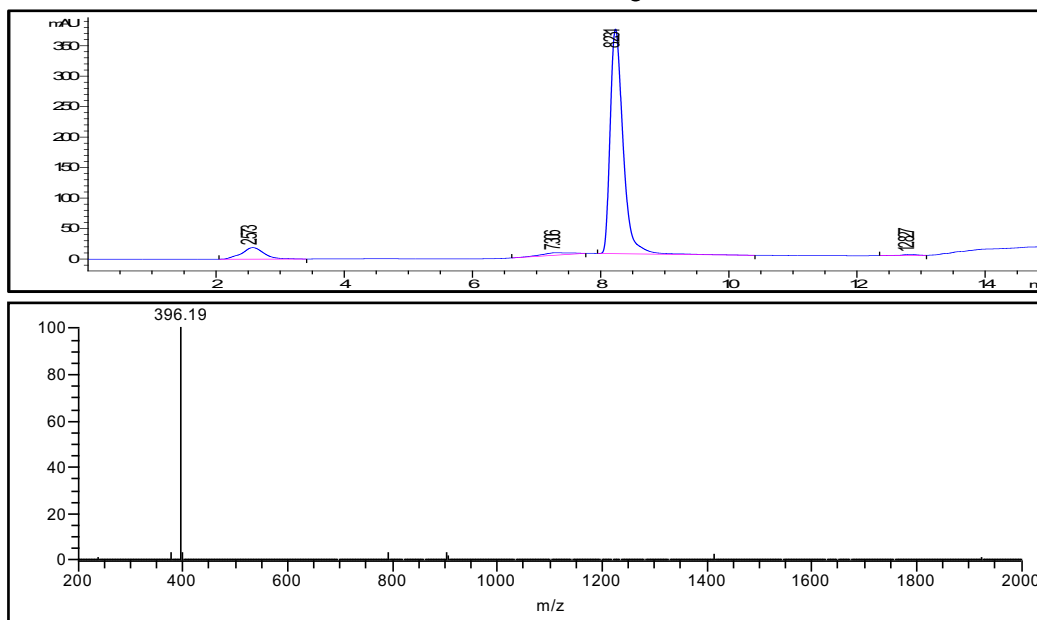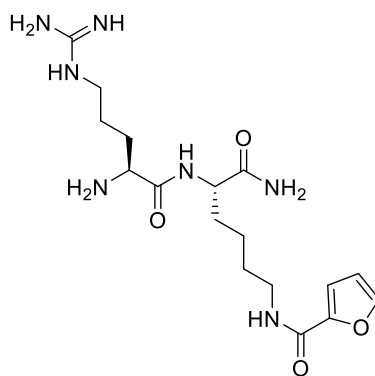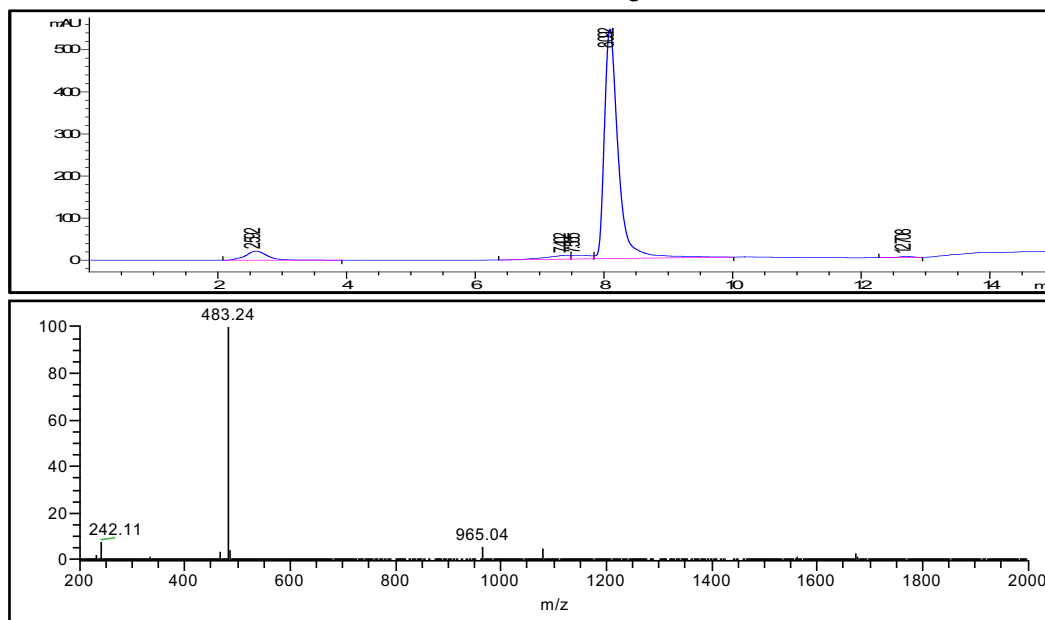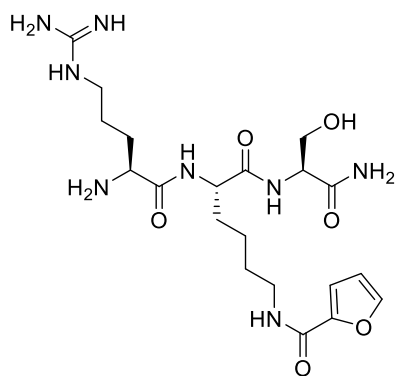
LC−MS analysis of peptide inhibitor XL-01:

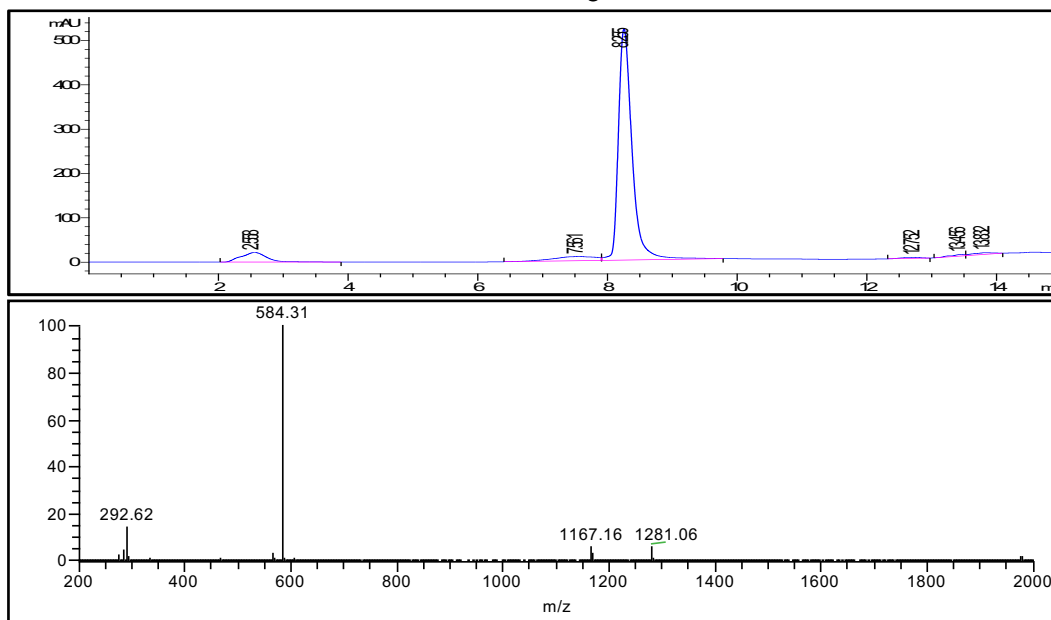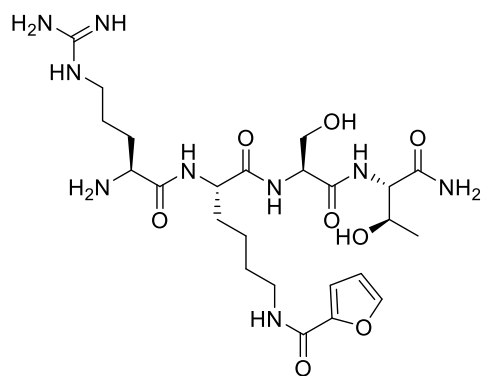Calculated m/z for $[M + H]^+$: 1154.58, found: 1154.61; calculated m/z for $[M + 2H]^{2+}$: 577.69, found: 578.05.
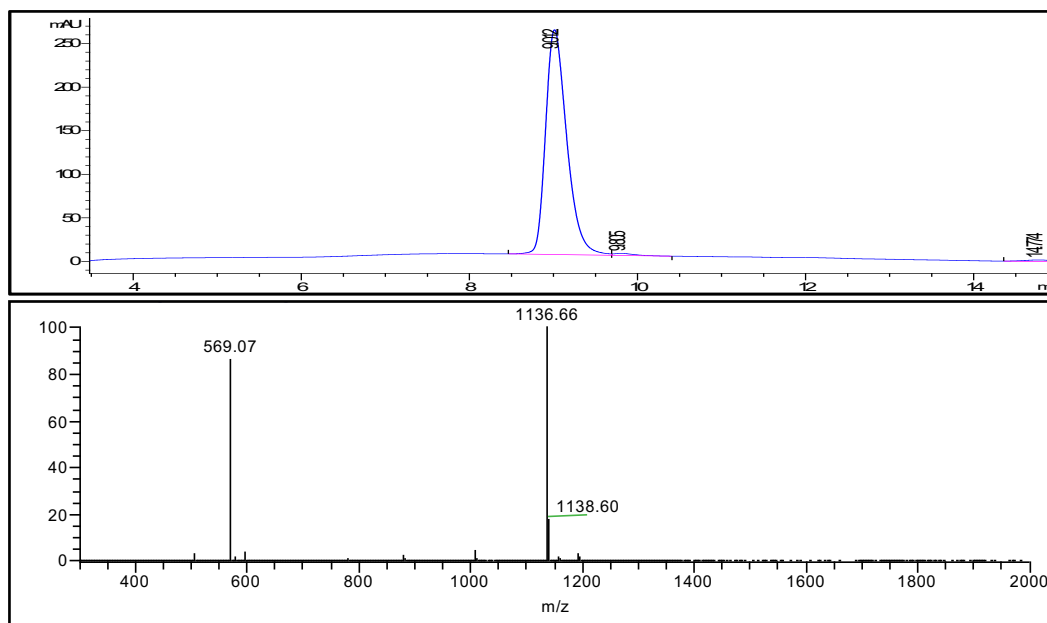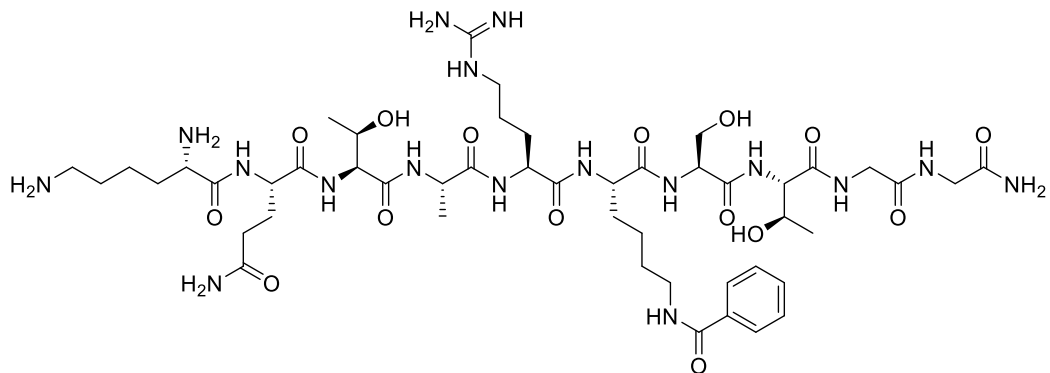
LC−MS analysis of peptide inhibitor XL-02:
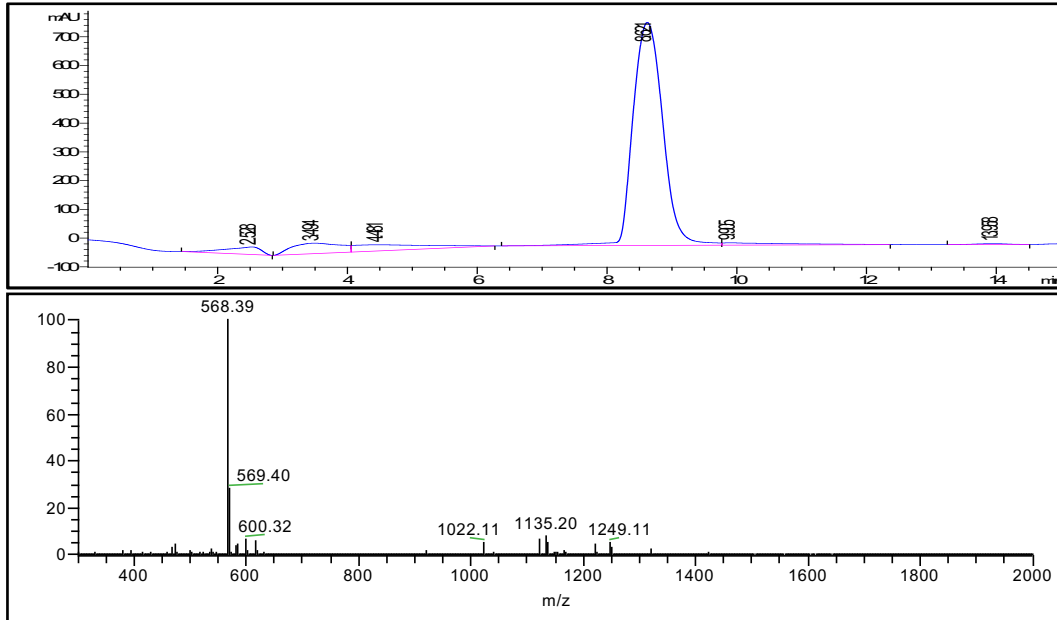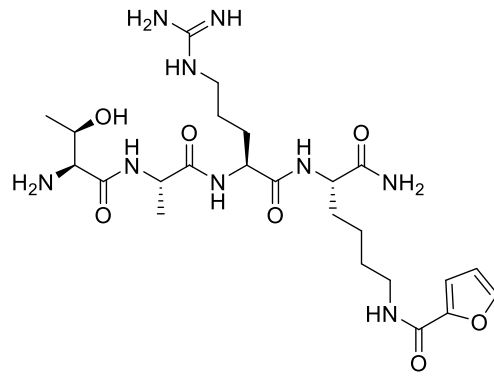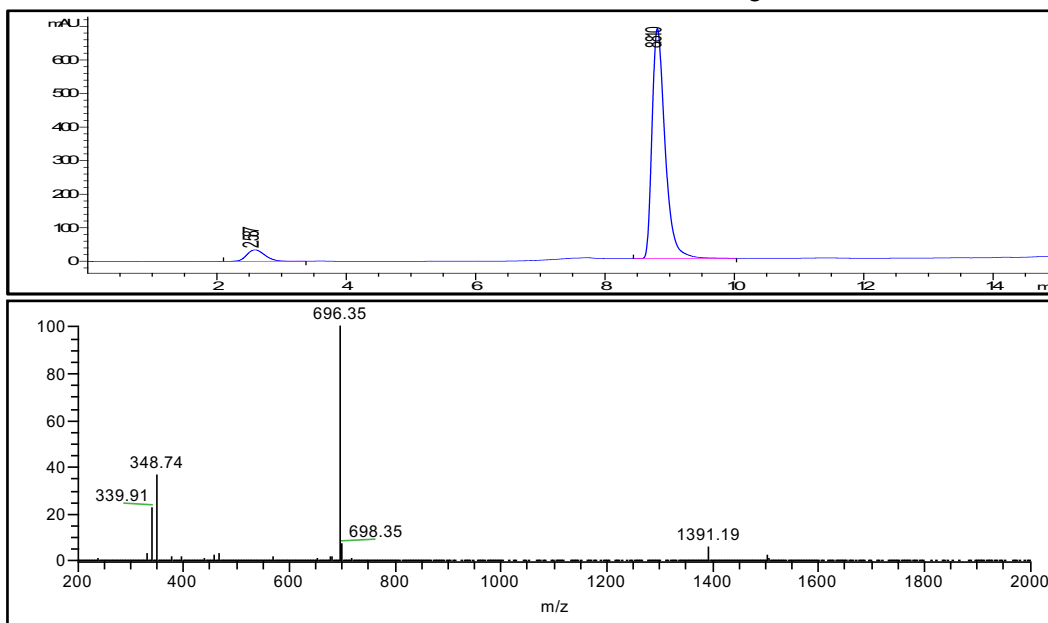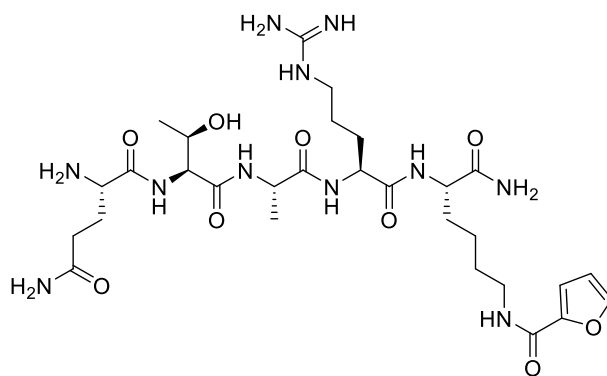
Calculated *m/z* for [M + H]$^+$: 1136.61, found: 1136.66; calculated *m/z* for [M + 2H]$^{2+}$: 568.81, found: 569.07.
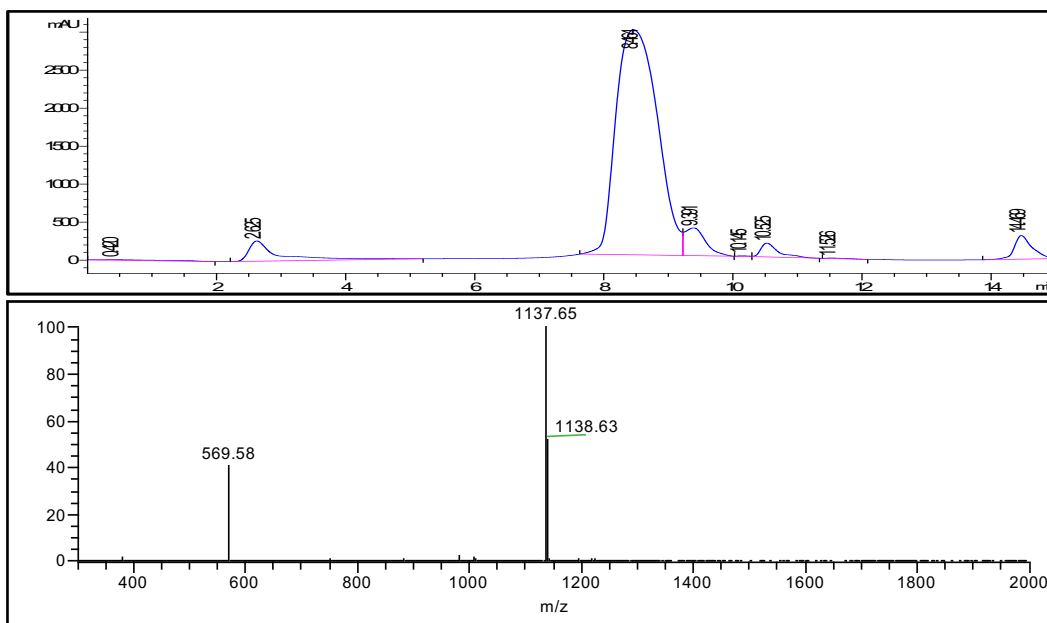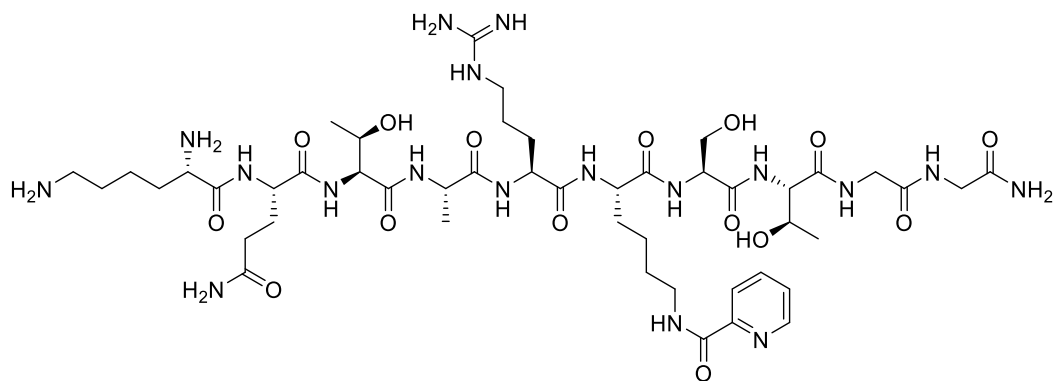
LC−MS analysis of peptide inhibitor XL-03:
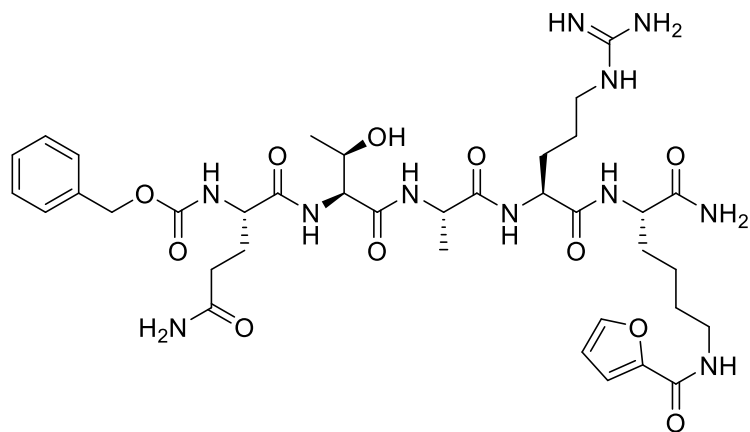
Calculated m/z for $[M + H]^+$: 1137.61, found: 1137.65; calculated m/z for $[M + 2H]^{2+}$: 569.31, found: 569.58.
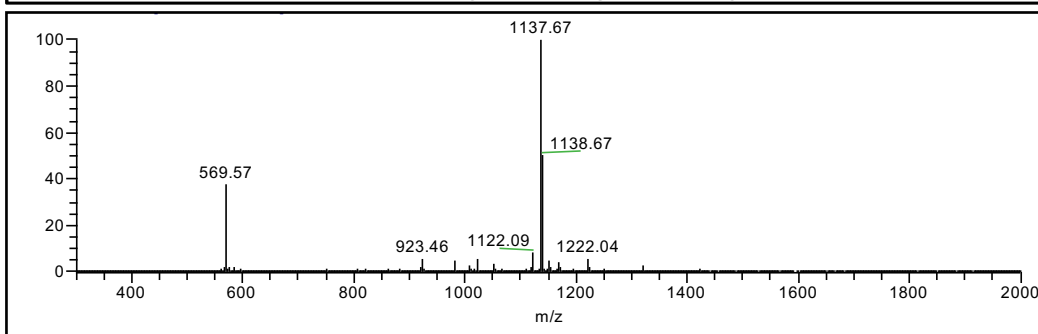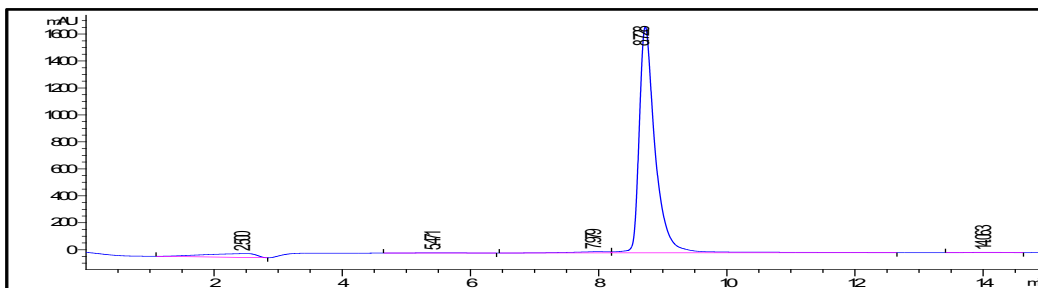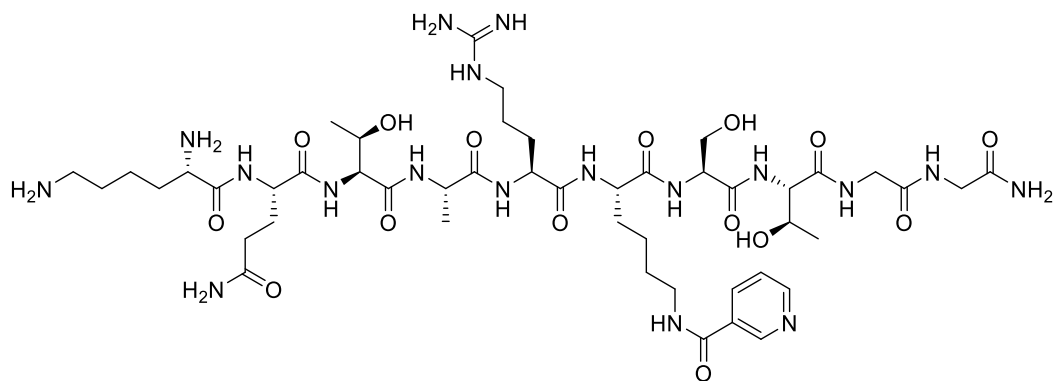
LC−MS analysis of peptide inhibitor XL-04:

Calculated m/z for $[M+H]^+$: 1137.61, found: 1137.67; calculated m/z for $[M+2H]^{2+}$: 569.31, found: 569.57.
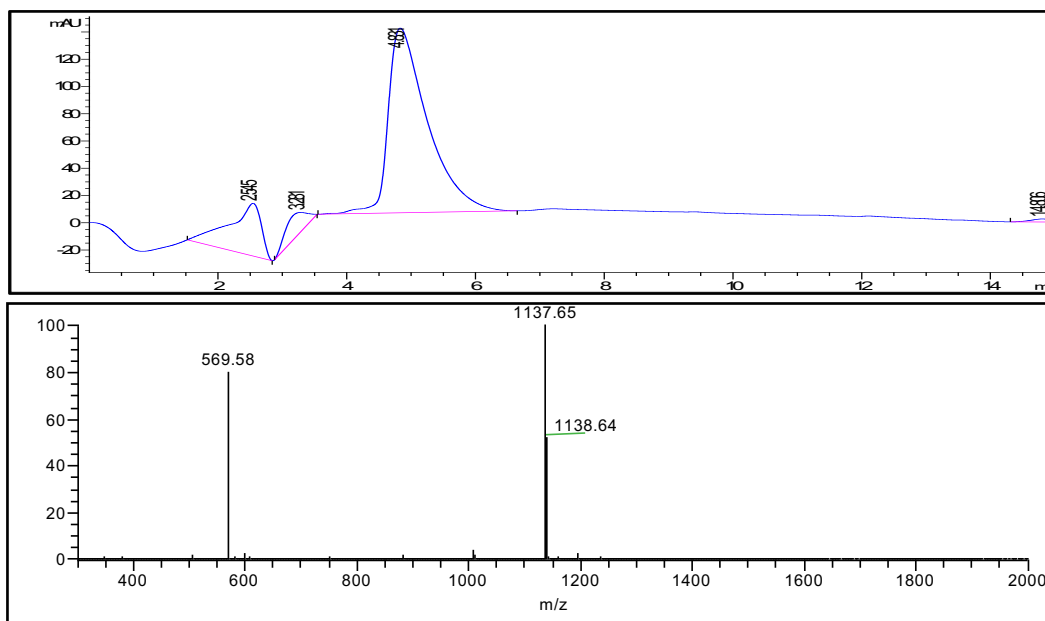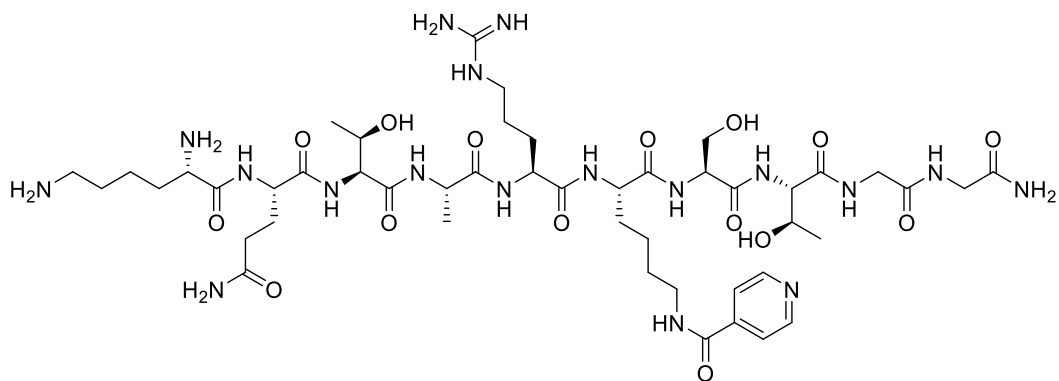
LC–MS analysis of peptide inhibitor XL-05:

Calculated m/z for $[M+H]^+$: 1137.61, found: 1137.65; calculated m/z for $[M+2H]^{2+}$: 569.31, found: 569.58.
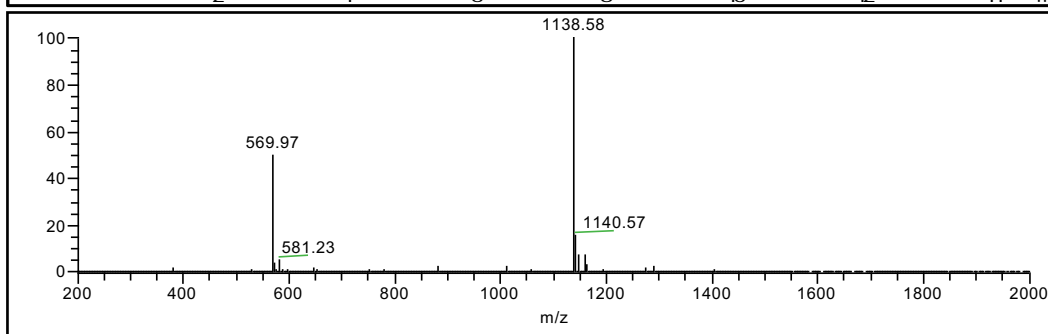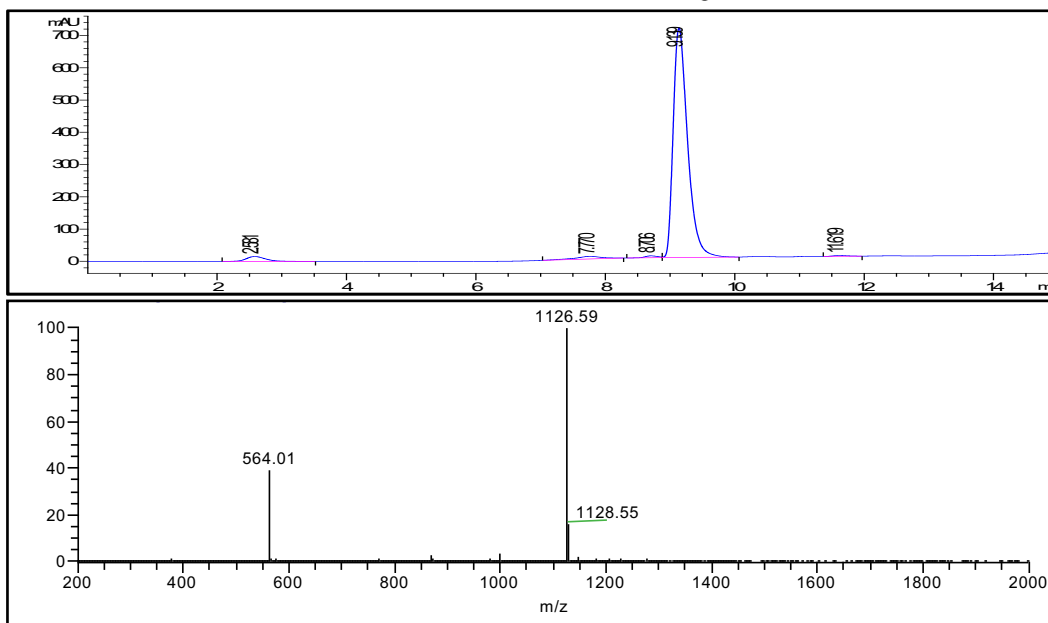
LC–MS analysis of peptide inhibitor XL-06:

Calculated m/z for $[M + H]^+$: 1138.60, found: 1138.58; calculated m/z for $[M + 2H]^{2+}$: 569.80, found: 569.97.

LC−MS analysis of peptide inhibitor XL-07:

Calculated *m/z* for [M + H]$^+$: 1126.59, found: 1126.63; calculated *m/z* for [M + 2H]$^{2+}$: 563.79, found: 564.06.
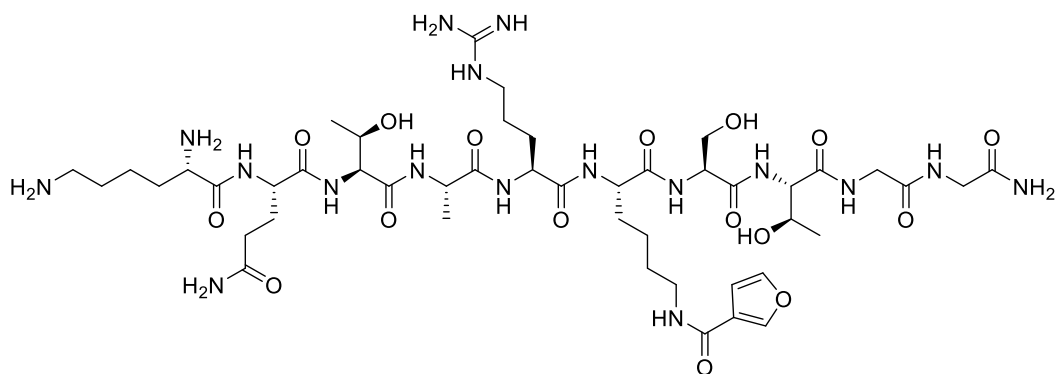
LC−MS analysis of peptide inhibitor XL-07a:

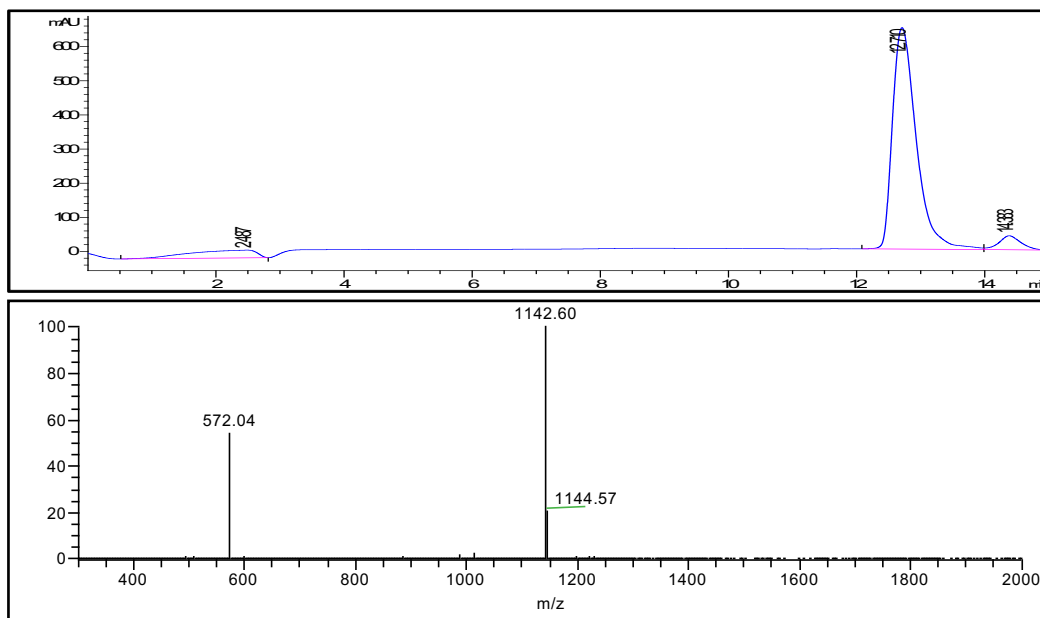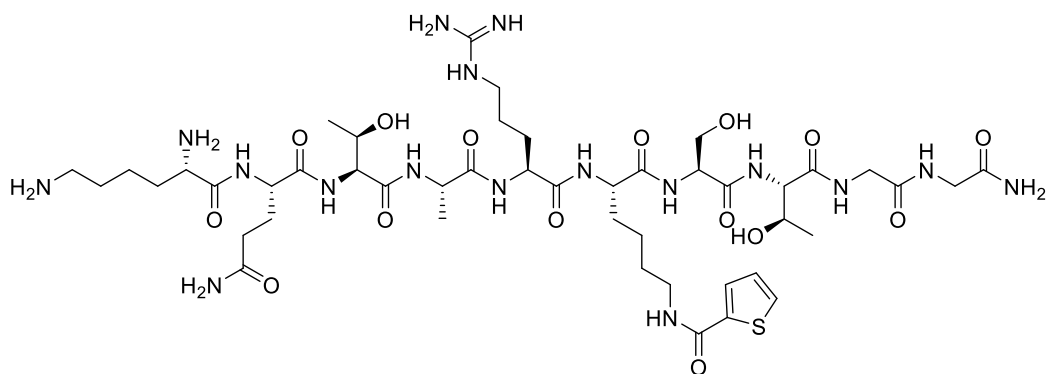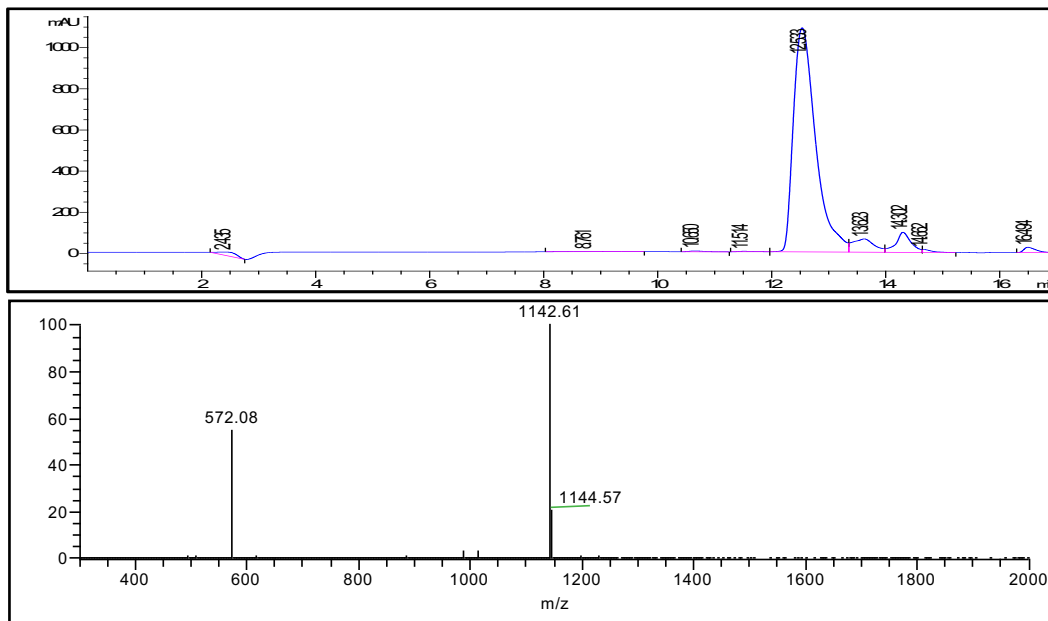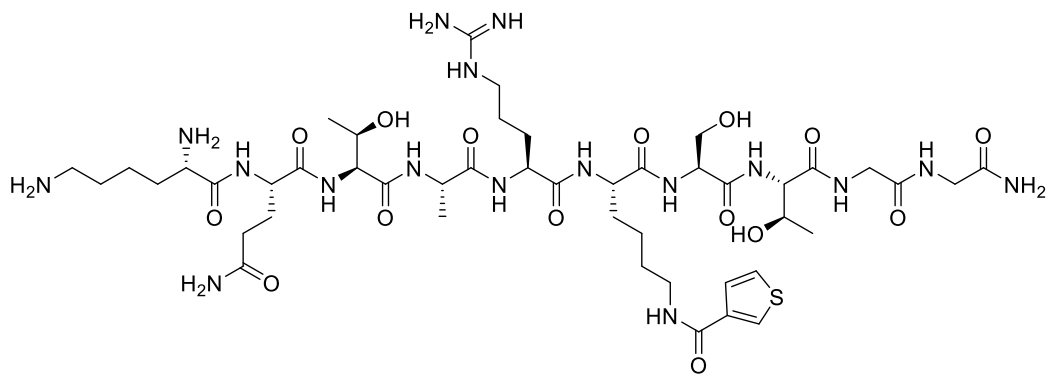Calculated m/z for $[M+H]^+$: 396.23, found: 396.19.

LC−MS analysis of peptide inhibitor XL-07b:

Calculated m/z for $[M + H]^{+}$: 483.27, found: 483.24.

LC−MS analysis of peptide inhibitor XL-07c:

Calculated m/z for $[M + H]^+$: 584.32, found: 584.31.

LC−MS analysis of peptide inhibitor XL-07d:

Calculated *m/z* for [M + H]$^+$: 467.27, found: 467.24.

LC−MS analysis of peptide inhibitor XL-07e:

Calculated *m/z* for [M + H]$^+$: 554.30, found: 554.27.

LC−MS analysis of peptide inhibitor XL-07f:

Calculated *m/z* for [M + H]$^+$: 655.35, found: 655.32.

LC−MS analysis of peptide inhibitor XL-07g:

Calculated m/z for $[M+H]^+$: 568.32, found: 568.39.

LC−MS analysis of peptide inhibitor XL-07h:

Calculated m/z for $[M+H]^+$: 696.38, found: 696.35.
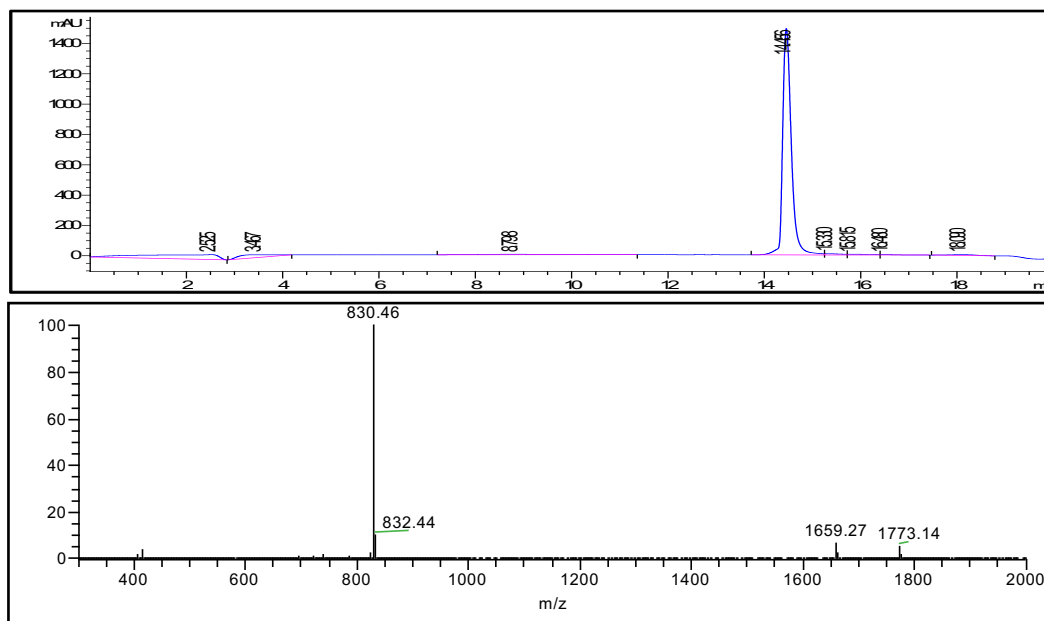
LC−MS analysis of peptide inhibitor XL-07i:

Calculated *m/z* for [M + H]⁺: 830.41, found: 830.46.

LC–MS analysis of peptide inhibitor XL-08:

Calculated *m/z* for [M + H]$^+$: 1126.59, found: 1126.59; calculated *m/z* for [M + 2H]$^{2+}$: 563.79, found: 564.01.

LC–MS analysis of peptide inhibitor XL-09:

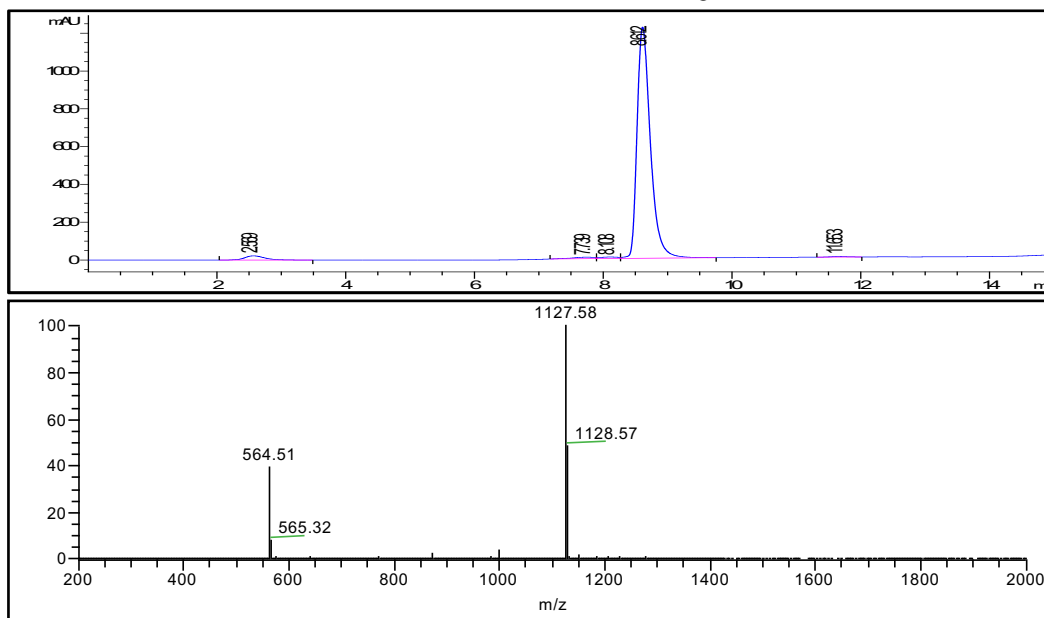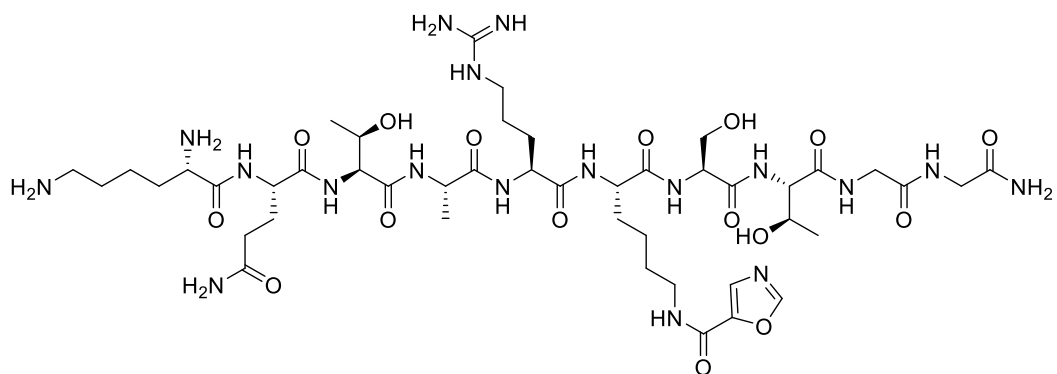Calculated *m/z* for [M + H]⁺: 1142.57, found: 1142.60; calculated *m/z* for [M + 2H]²⁺: 571.78, found: 572.04.

LC−MS analysis of peptide inhibitor XL-10:

Calculated m/z for $[M+H]^+$: 1142.57, found: 1142.61; calculated m/z for $[M+2H]^{2+}$: 571.78, found: 572.08.
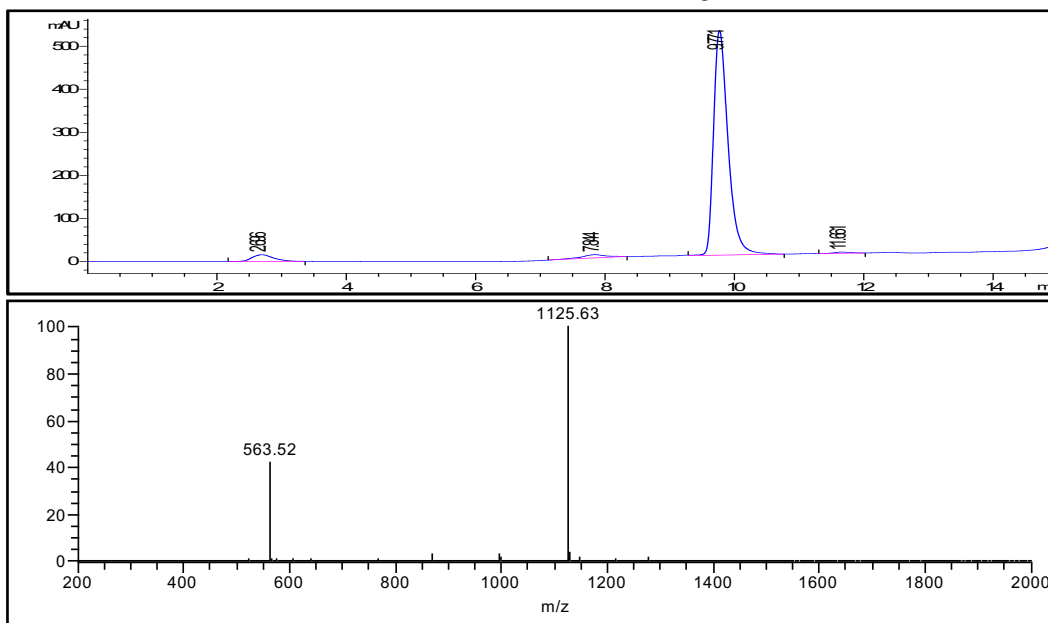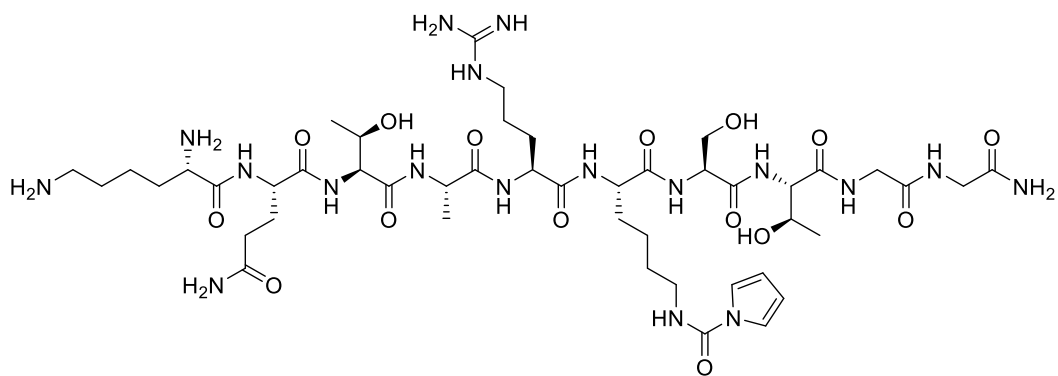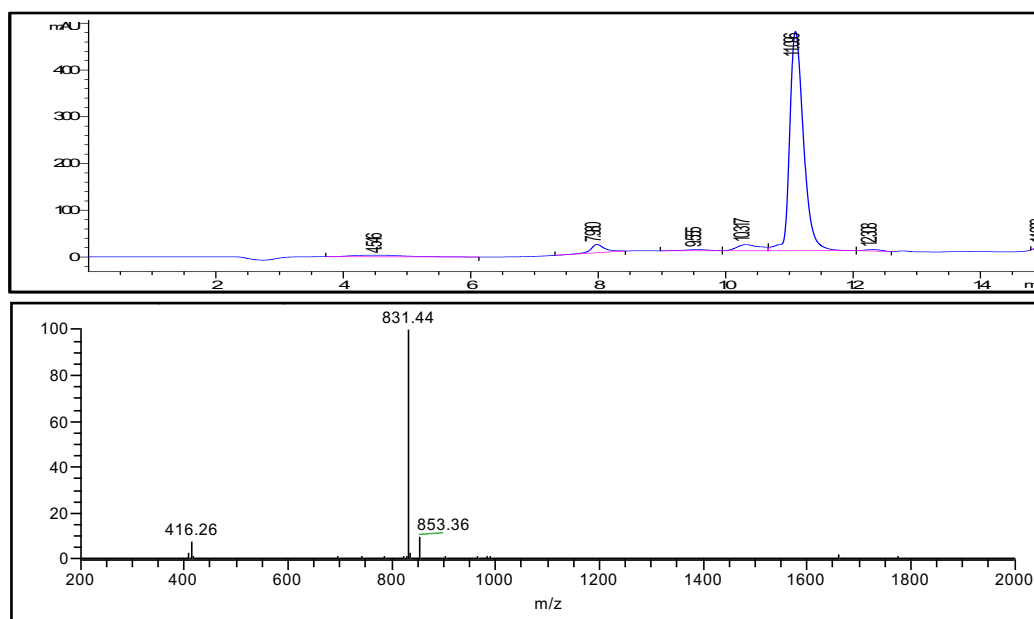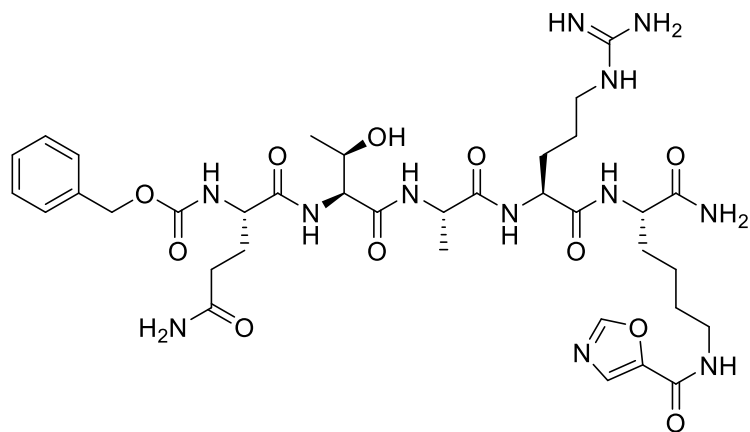
LC−MS analysis of peptide inhibitor XL-11:

Calculated *m/z* for [M + H]⁺: 1125.61, found: 1125.63; calculated *m/z* for [M + 2H]²⁺: 563.30, found: 563.52.
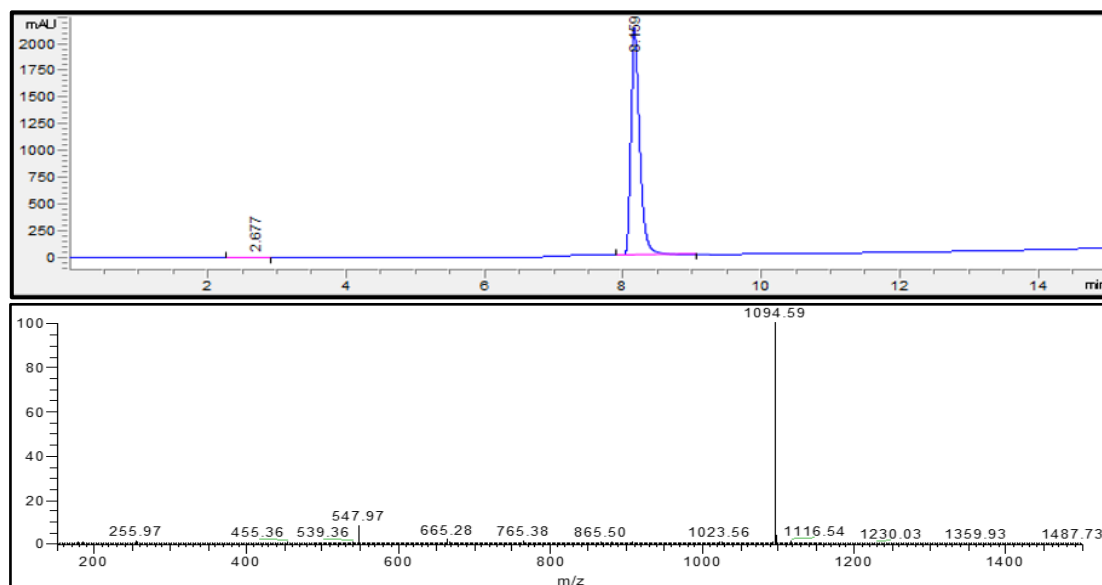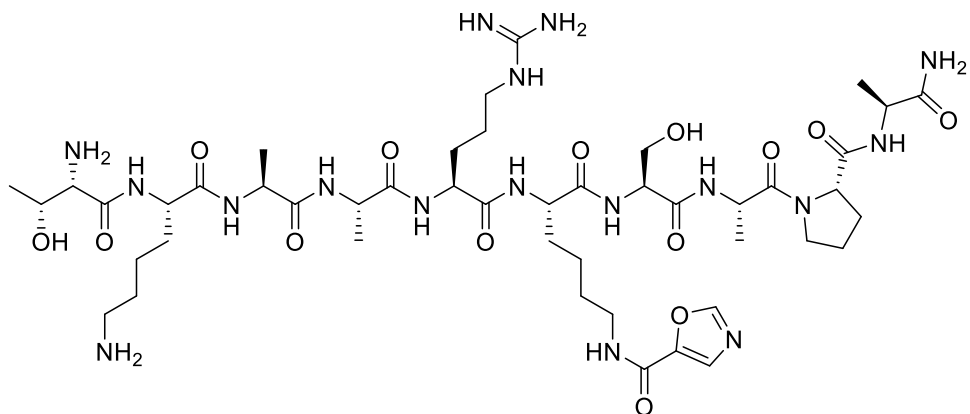
LC−MS analysis of peptide inhibitor XL-12:

Calculated m/z for $[M + H]^+$: 1127.58, found: 1127.56; calculated m/z for $[M + 2H]^{2+}$: 564.29, found: 564.48.

LC−MS analysis of peptide inhibitor XL-13:

Calculated *m/z* for [M + H]⁺: 1127.58, found: 1127.58; calculated *m/z* for [M + 2H]²⁺: 564.29, found: 564.51.

LC−MS analysis of peptide inhibitor XL-13a:

Calculated *m/z* for [M + H]$^+$: 831.40, found: 831.44.

LC−MS analysis of probe XL-13b:

Calculated m/z for $[M+H]^+$: 1195.65, found: 1195.65; calculated m/z for $[M+2H]^{2+}$: 598.32, found 598.56.
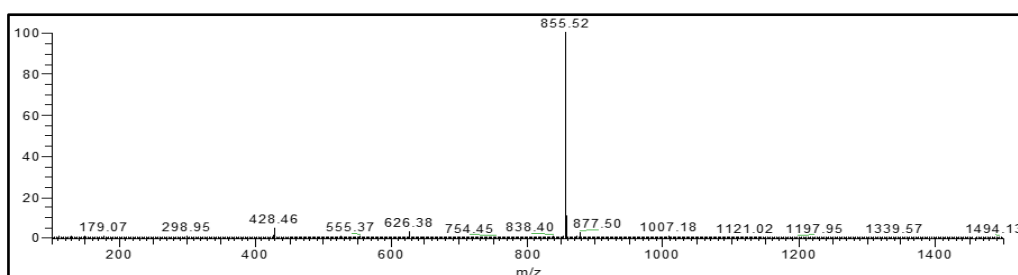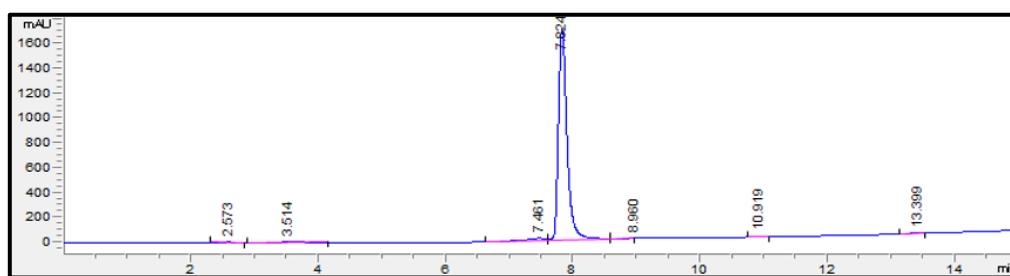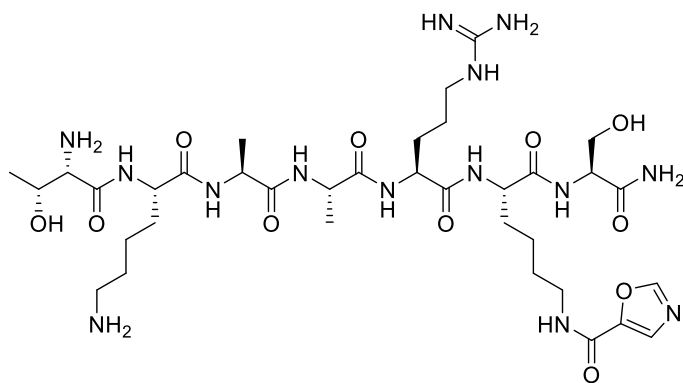
LC–MS analysis of probe XL-13c:

Calculated m/z for $[M + H]^+$: 1094.60, found: 1094.59; calculated m/z for $[M + 2H]^{2+}$: 548.80, found 547.97.

LC–MS analysis of probe XL-13d:

Calculated *m/z* for [M + H]$^+$: 1023.56, found: 1023.61; calculated *m/z* for [M + 2H]$^{2+}$: 512.28, found 512.43.
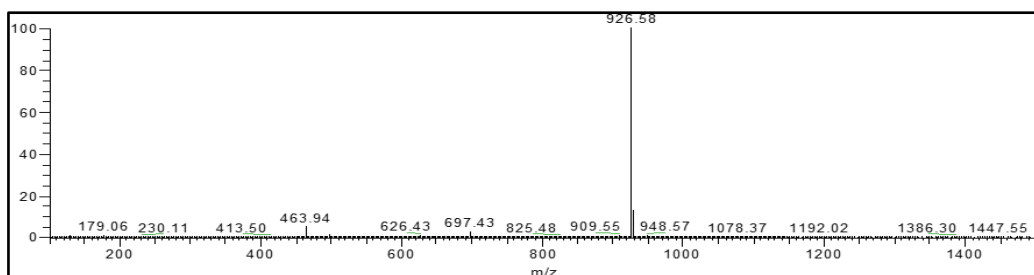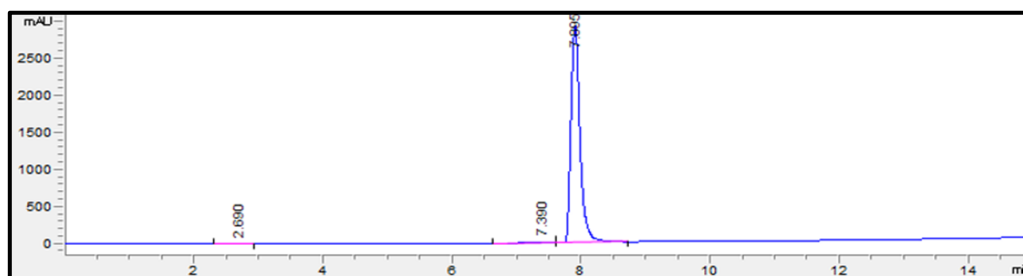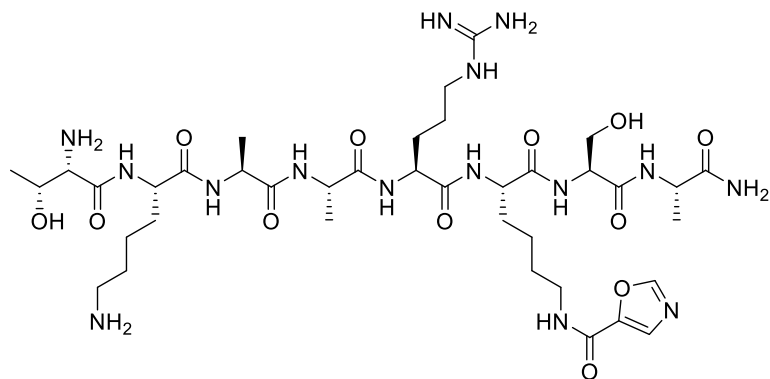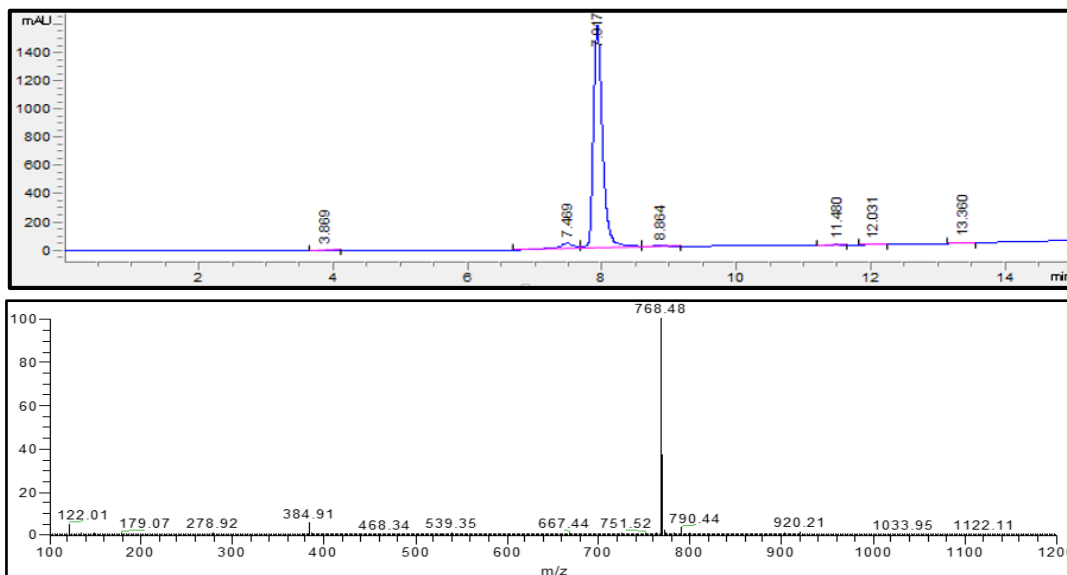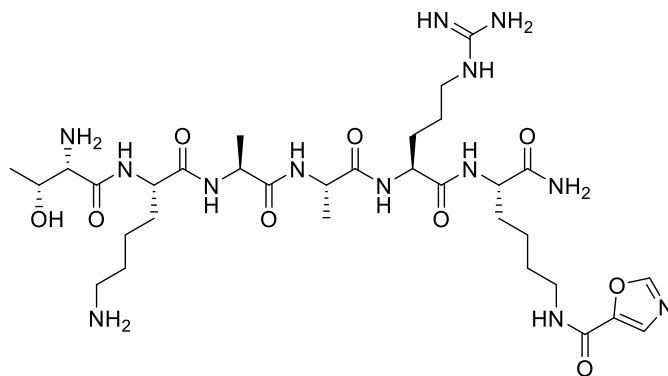
LC–MS analysis of probe XL-13e:

Calculated m/z for $[M + H]^+$: 926.51, found: 926.58; calculated m/z for $[M + 2H]^{2+}$: 463.76, found 463.94.
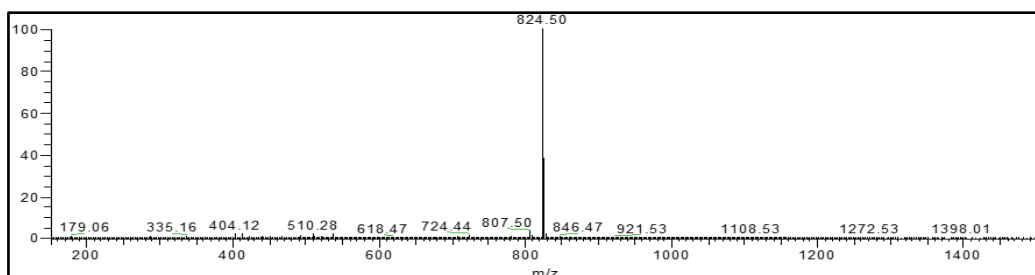
LC–MS analysis of probe XL-13f:
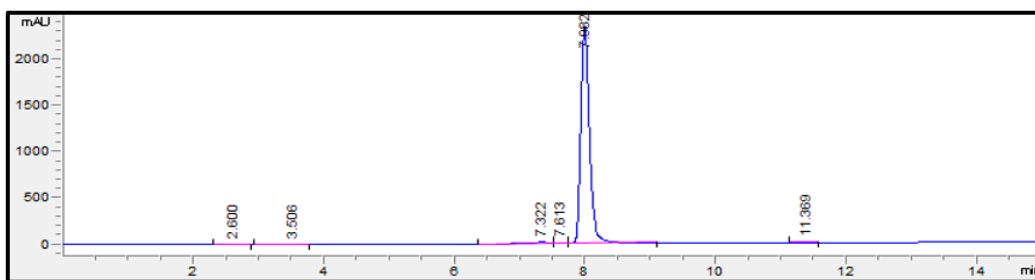
Calculated *m/z* for [M + H]$^+$: 855.47, found: 855.52; calculated *m/z* for [M + 2H]$^{2+}$: 428.24, found 428.46.

LC–MS analysis of probe XL-13g:

Calculated *m/z* for [M + H]$^+$: 768.44, found: 768.48.

LC−MS analysis of probe XL-13h:

Calculated *m/z* for [M + H]$^+$: 824.43, found: 824.50.

LC–MS analysis of probe XL-13i:

Calculated *m/z* for [M + H]⁺: 895.47, found: 895.51.

LC–MS analysis of probe XL-13j:

Calculated m/z for $[M+H]^+$: 966.50, found: 966.55.

LC–MS analysis of probe XL-13k:

Calculated m/z for $[M + H]^+$: 1094.60, found: 1094.66; calculated m/z for $[M + 2H]^{2+}$: 547.80, found 547.96.
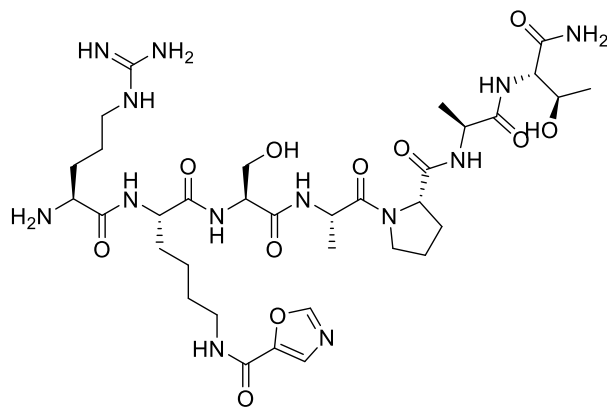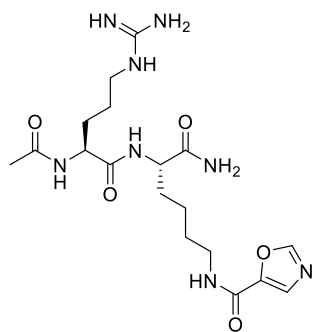
LC−MS analysis of probe XL-13l:

Calculated *m/z* for [M + H]⁺: 439.23, found: 439.27; calculated *m/z* for [2M + H]⁺: 877.46, found 876.92.

LC−MS analysis of probe XL-13m:

Calculated *m/z* for [M + H]$^+$: 510.27, found: 510.29; calculated *m/z* for [2M + H]$^+$: 1019.54, found 1019.16.
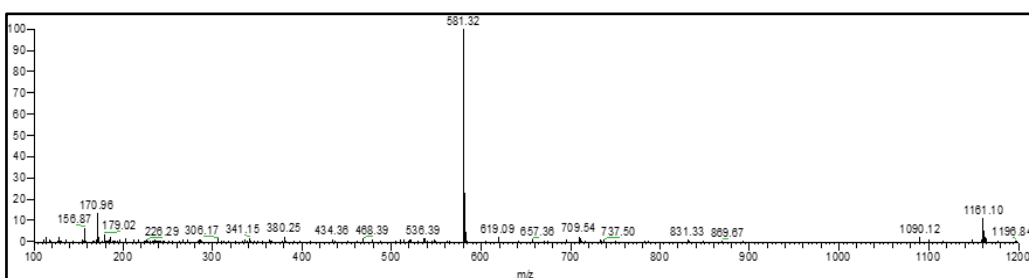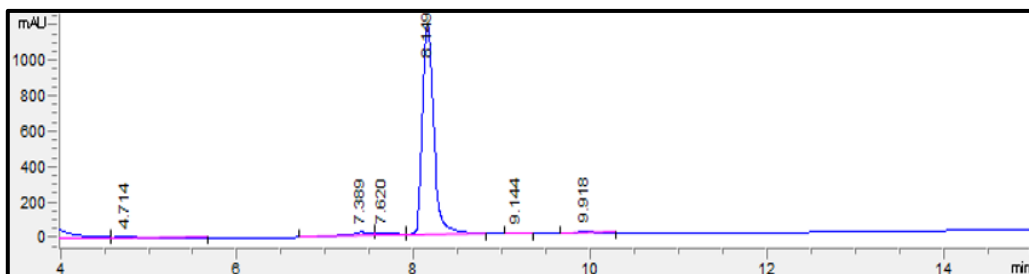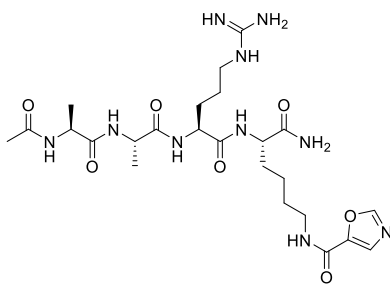
LC−MS analysis of probe XL-13n:

Calculated *m/z* for [M + H]⁺: 581.32, found: 581.32; calculated *m/z* for [2M + H]⁺: 1161.64, found 1161.10.
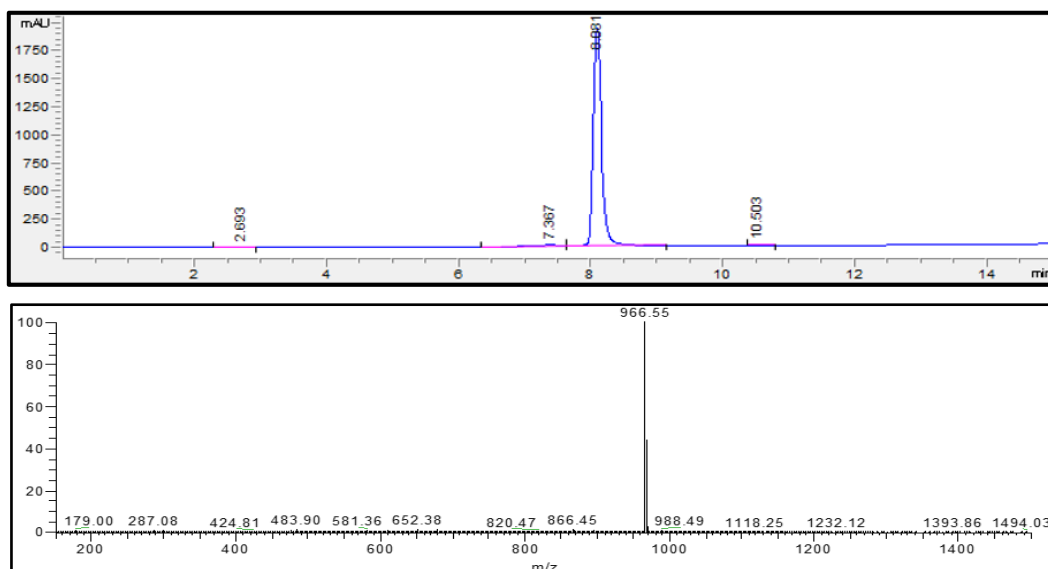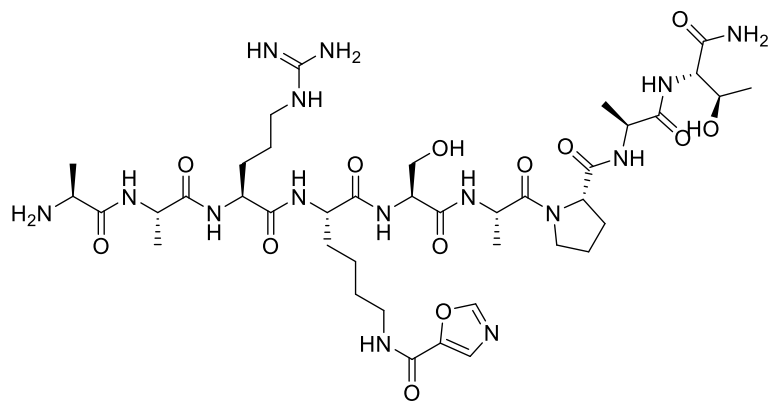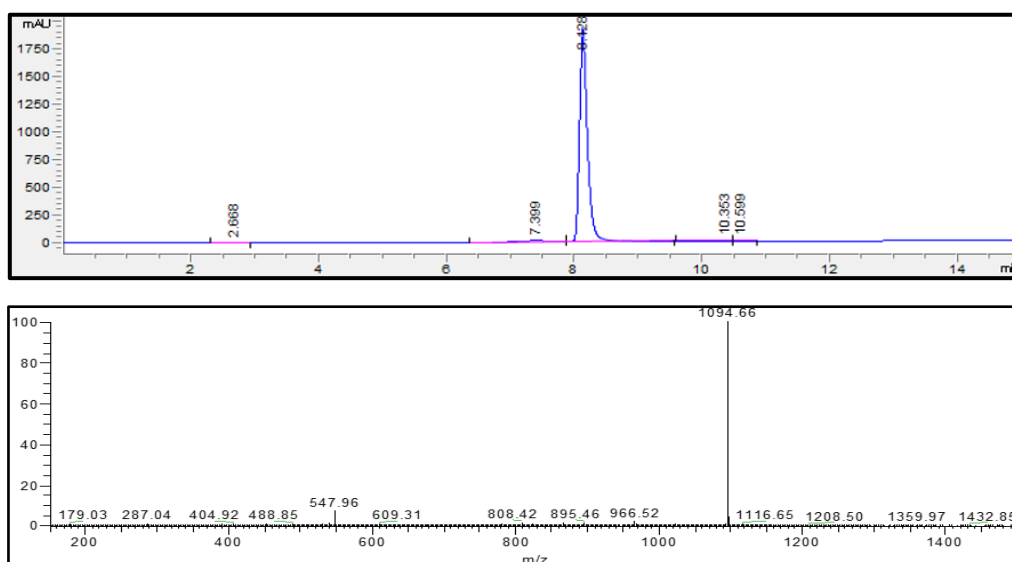
LC−MS analysis of probe XL-13n:

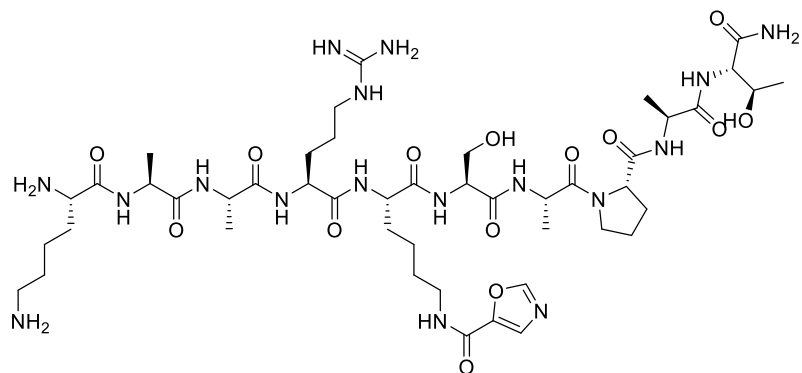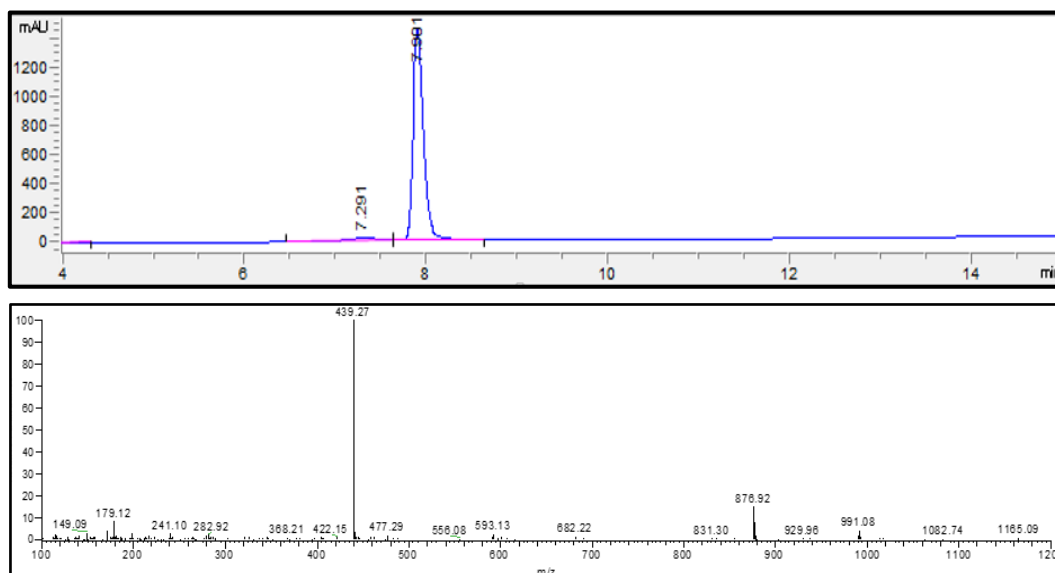Calculated m/z for $[M+H]^+$: 709.40, found: 709.48.

LC–MS analysis of peptide inhibitor XL-14:

Calculated m/z for $[M + H]^+$: 1127.58, found: 1127.58; calculated m/z for $[M + 2H]^{2+}$: 564.29, found: 564.50.
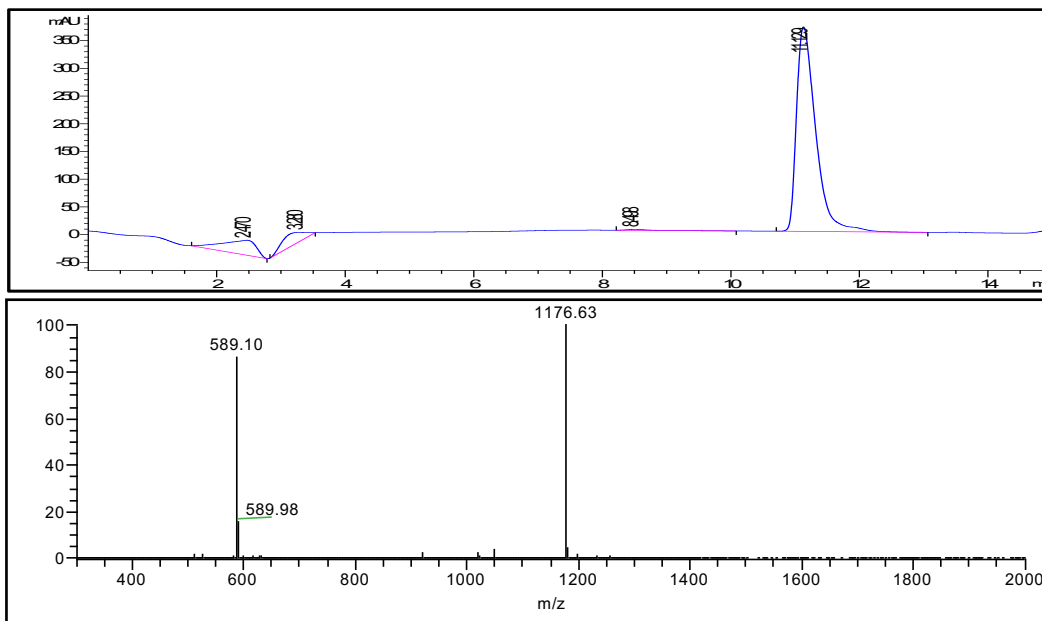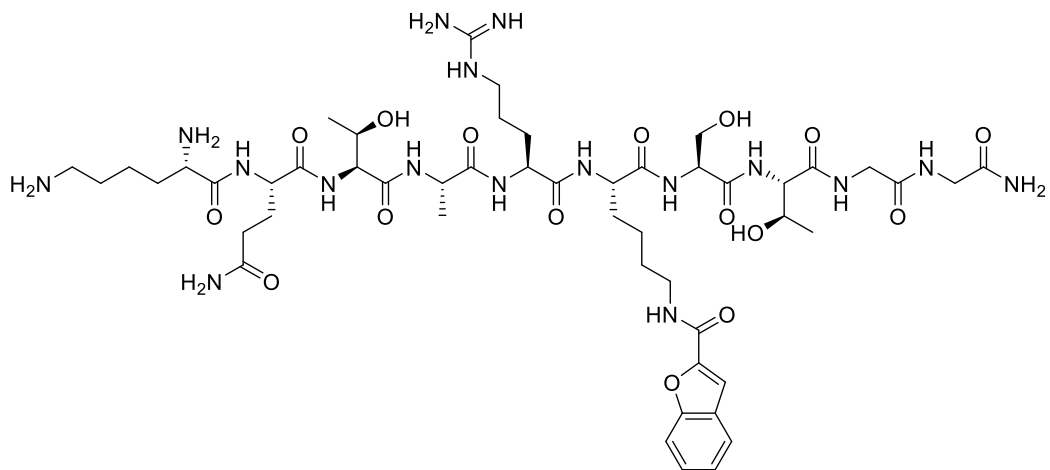
LC−MS analysis of peptide inhibitor XL-15:

Calculated m/z for $[M+H]^+$: 1176.60, found: 1176.63; calculated m/z for $[M+2H]^{2+}$: 588.80, found: 589.10.
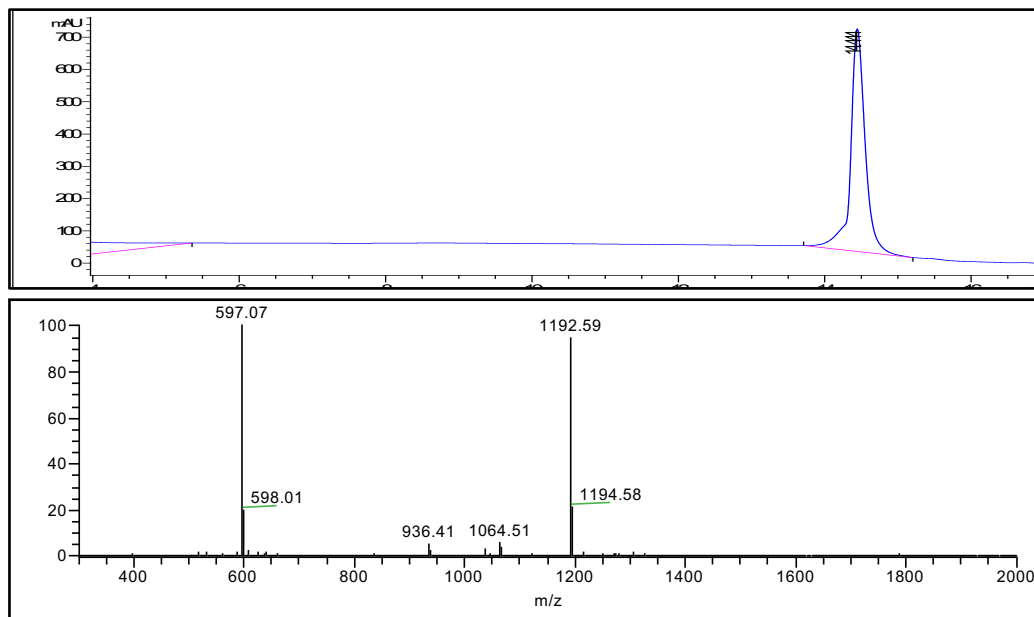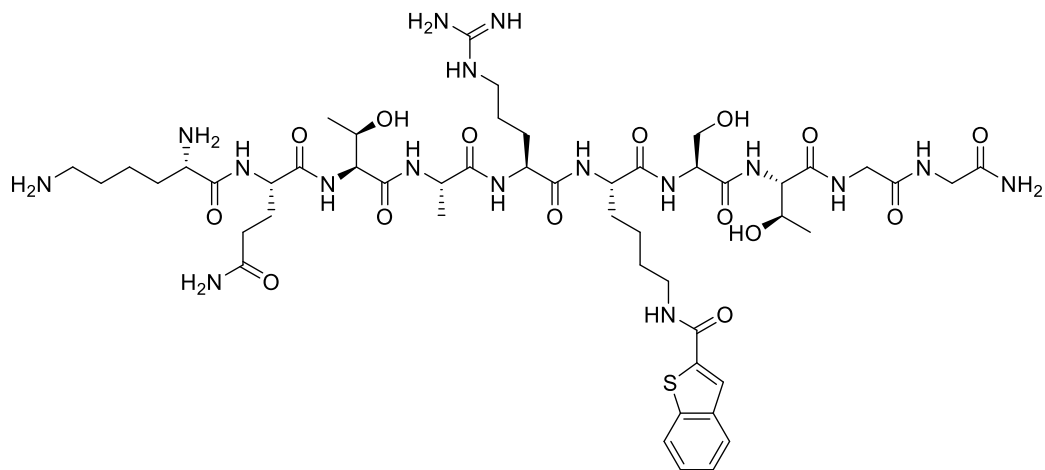
LC−MS analysis of peptide inhibitor XL-16:

Calculated m/z for $[M + H]^+$: 1192.58, found: 1192.59; calculated m/z for $[M + 2H]^{2+}$: 596.79, found: 597.07.
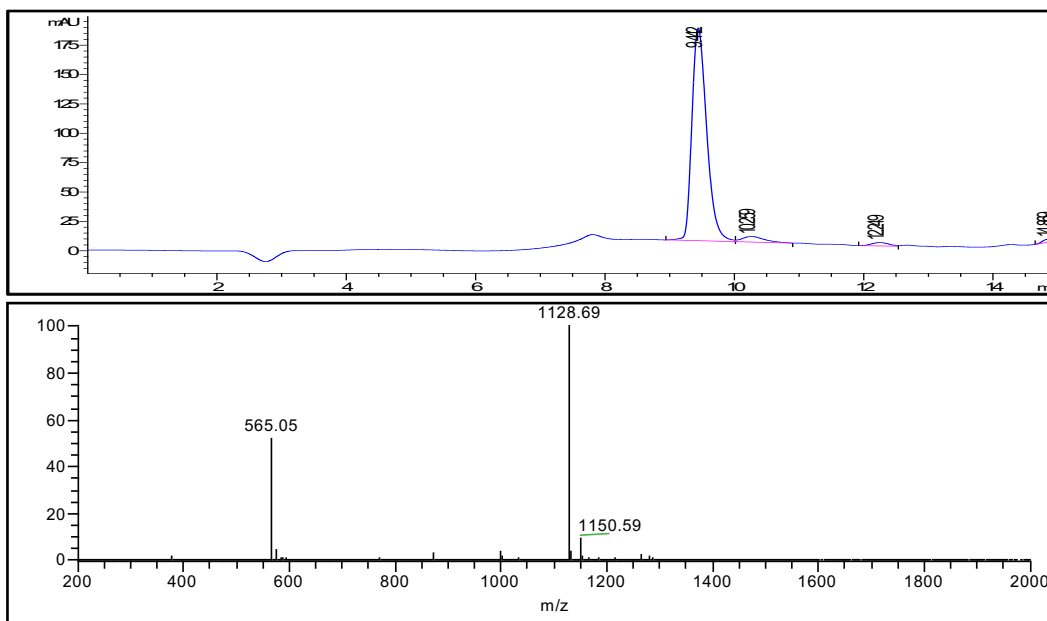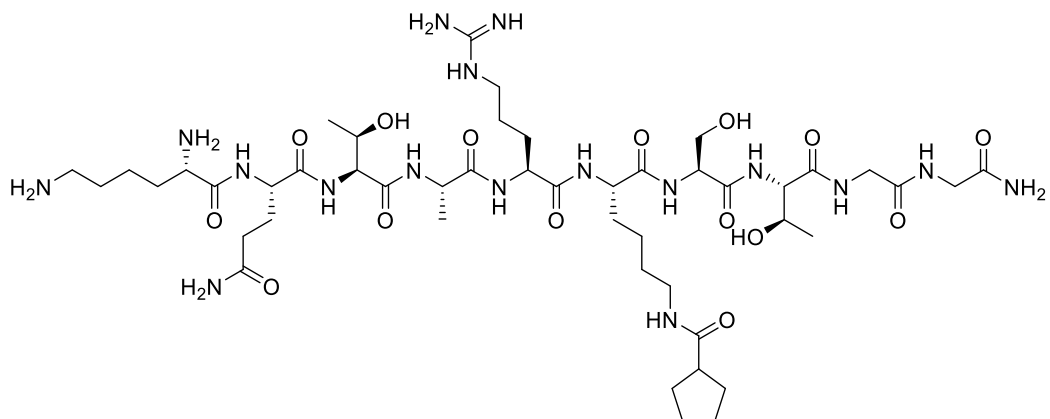
LC−MS analysis of peptide inhibitor XL-17:

Calculated *m/z* for [M + H]$^+$: 1128.64, found: 1128.69; calculated *m/z* for [M + 2H]$^{2+}$: 564.82, found: 565.05.
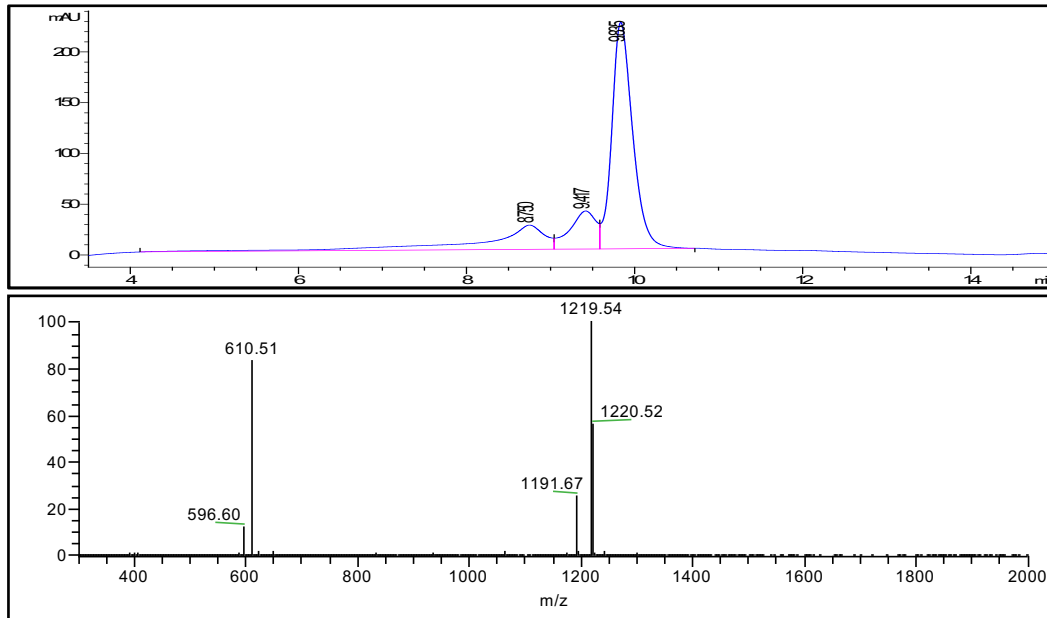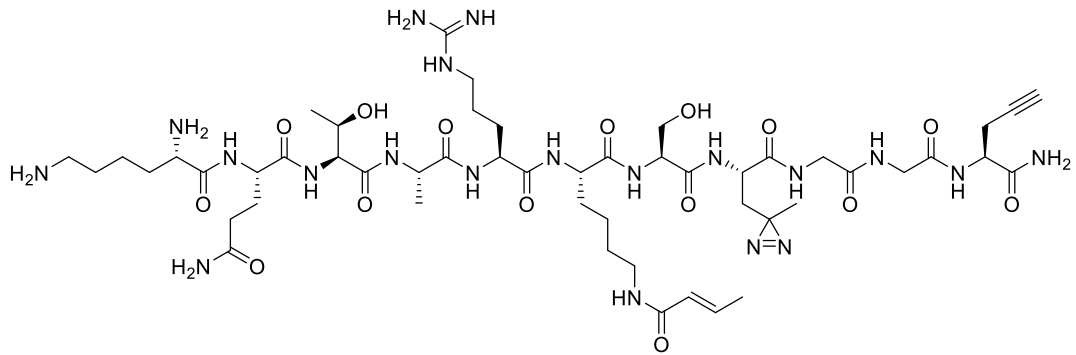
LC−MS analysis of photo-H3K9cr:

Calculated m/z for $[M + H]^+$: 1219.66, found: 1219.54; calculated m/z for $[M + H − N_2]^+$: 1191.66, found: 1191.67; calculated m/z for $[M + 2H]^{2+}$: 610.33, found: 610.51.
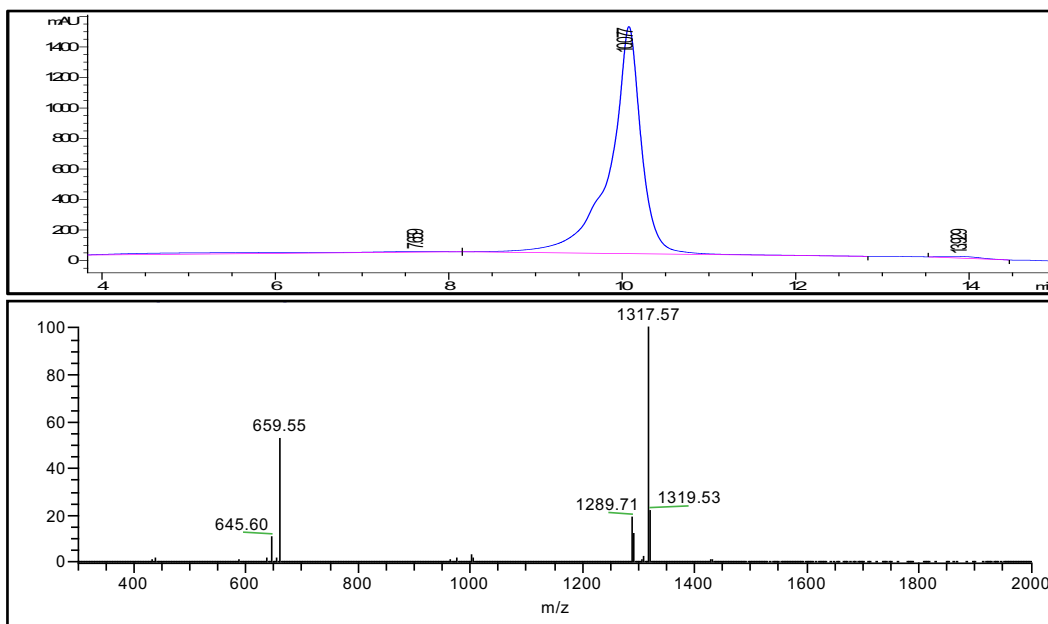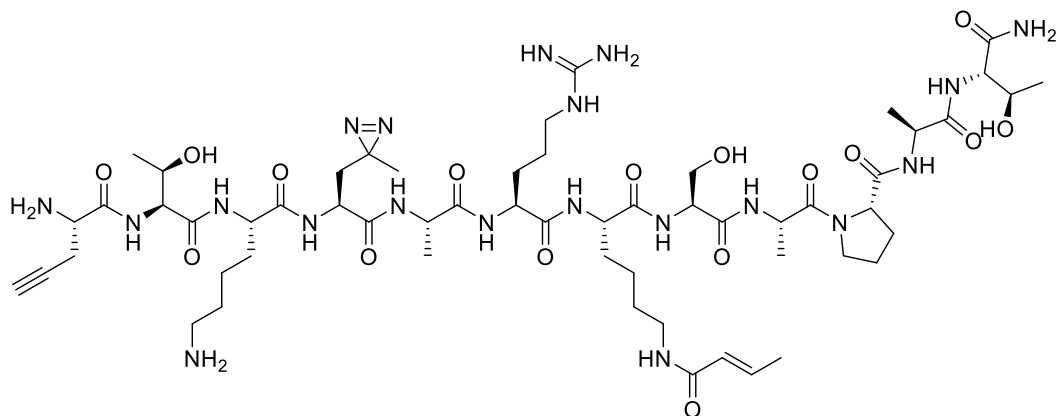
LC−MS analysis of photo-H3K27cr:

Calculated m/z for $[M + H]^+$: 1317.73, found: 1317.57; calculated m/z for $[M + H - N_2]^+$: 1289.73, found: 1289.71; calculated m/z for $[M + 2H]^{2+}$: 659.37, found: 659.55.

Supplementary Table 1 Data collection and refinement statistics (molecular replacement)

	AF9 YEATS/XL-07i
Data collection	
Space group	C121
Cell dimensions	
a, b, c (Å)	91.54, 43.99, 89.05
α, β, γ (°)	90.00, 95.86, 90.00
Resolution (Å)	50.00-1.90(1.93-1.90)*
R_{sym} or R_{merge}	10.2(89.7)
$I / \sigma I$	25.78(2.59)
Completeness (%)	99.8(99.9)
Redundancy	5.1(5.1)
Refinement	
Resolution (Å)	42.29-1.90(1.97-1.90)
No. reflections	27,771
R_{work} / R_{free}	20.2/22.4
No. atoms	
Protein	2,427
Ligand/ion	15
Water	278
B-factors	
Protein	34.3
Ligand/ion	43.7
Water	40.5
R.m.s. deviations	
Bond lengths (Å)	0.008
Bond angles (°)	0.861

* The data set was collected and processed based on one crystal. Highest-resolution shell is shown in parentheses.

Supplementary Table 2 Primers used in this study.

Gene	Sequence 5'-3'	Application
HOXA10[a]	F: GCCGCTCTCGAGTAAGGTAC	ChIP-qPCR
	R: GGCAAAGAGTGGTCGGAAGA	
	F: CTTTCGCGCAGAACATCAAAG	qPCR
	R: CCGCTCTCGAGTAAGGTACATA	
MEIS1[a]	F: AAGGGGCTGTGAAACTAGGC	ChIP-qPCR
	R: CTCCCGAGGGTAGAAGGTGA	
	F: CCAGCATCTAACACACCCTTAC	qPCR
	R: TATGTTGCTGACCGTCCATTAC	
MYB[a]	F: TGTTTCAGCCCACGTCTACC	ChIP-qPCR
	R: GACGCTTTCCAGACTTGGGA	
	F: CTCCAAGAACTCCTACACCATTC	qPCR
	R: GTCATCTGCTCCTCCATCTTTC	
MYC[a]	F: CATGCCATAACCCAGCTGTCT	ChIP-qPCR
	R: CACCCTTACTCCTCTCACCATGA	
	F: CACCGAGTCGTAGTCGAGGT	qPCR
	R: TTTCGGGTAGTGGAAAACCA	
HOXA9[a]	F: TACGTGGACTCGTTCCTGCT	qPCR
	R: CGTCGCCTTGGACTGGAAG	
CDC25A	F: CAGTCTTTATCCCTGGCATCTT	qPCR
	R: CAGTAGGTACAATGGGCTTCTT	
CDT1	F: CCGGGCCAGAAGATAAAGAAA	qPCR
	R: CTCGATGGTGAGCTGGTAATC	
CENPM	F: GAACACGGCCACCATCTT	qPCR
	R: CTCTGTGTTCTGGAGACTGTATTT	
MCM4	F: GGGCAGCAGCAGAAGATATAG	qPCR
	R: CCTGTGGGTAAGAGATGAGTTG	
MYBL2	F: CTGGAACAAACAGGACACATTG	qPCR
	R: GTGAGGCTGGAAGAGTTTGA	
TERT	F: GGTGAACTTCCCTGTAGAAGAC	qPCR
	R: GGTTCTTCCAAACTTGCTGATG	
TSPOAP1	F: CCTGATGCTGGAGAAGAAGAG	qPCR
	R: CTGAGCCCTCAAGGAGAATATC	
B2M[a]	F: TCTCTGCTGGATGACGTGAG	qPCR
	R: TAGCTGTGCTCGCGCTACT	

[a]Reference: M.A. Erb *et al.*, *Nature*, **2017**, 543, 270-274.
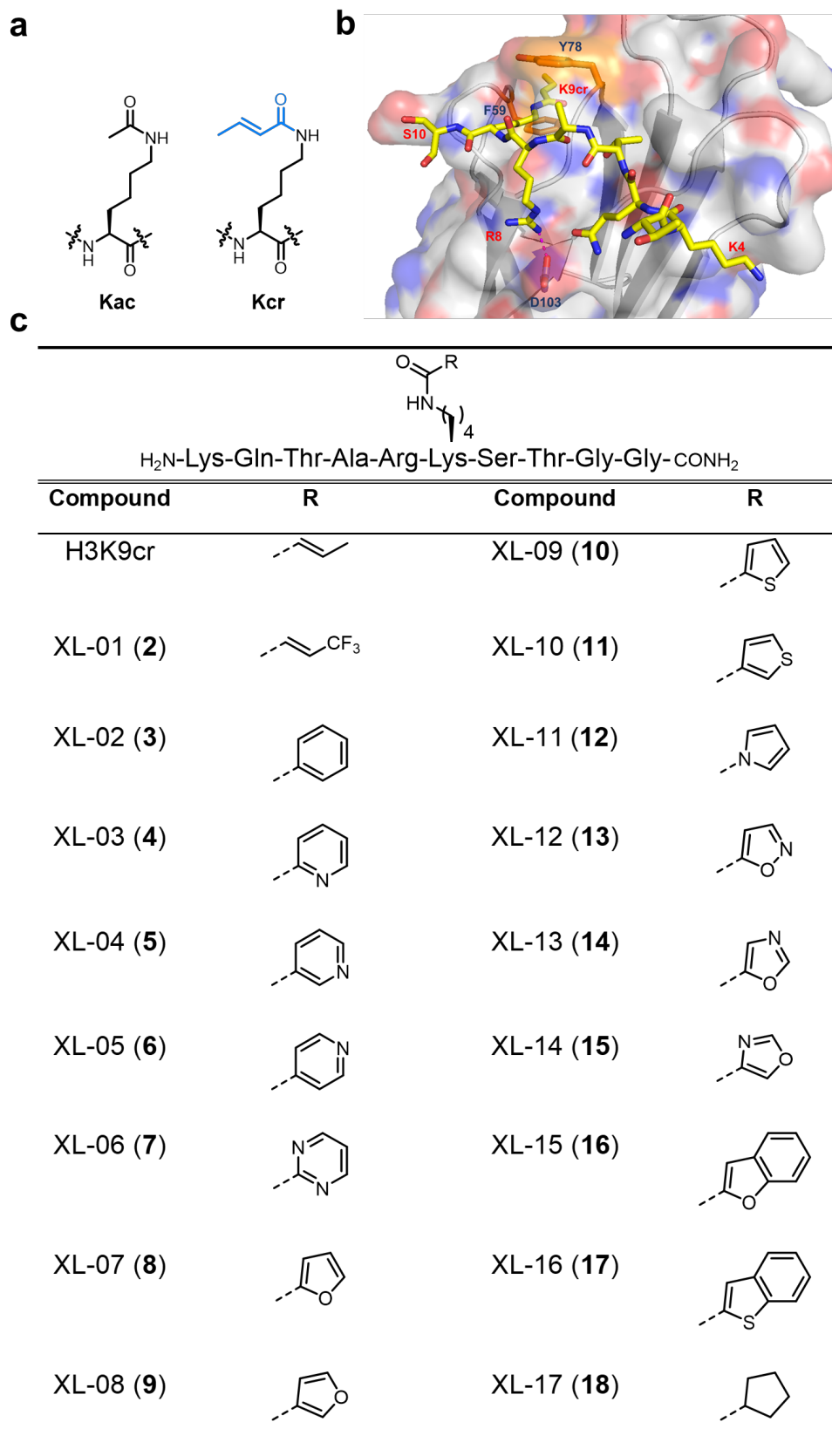
Supplementary Figure 1. Design of YEATS domain by targeting the π- π-π stacking. (**a**) Structure of lysine acetylation (Kac) and crotonylation (Kcr). (**b**) Crystal structure of AF9 YEATS domain in complex with H3K9cr peptide. The structure was accessed from RSCB Protein Data Band (PDB code 5HJB) and processed by PyMol. Protein (grey) was showed using surface mode with 15% transparency. The H3K9cr peptide (yellow) was showed in stick. The Y78 and F59 of AF9 were highlighted in orange. The hydrogen bond between D103 and H3R8 was indicated with dashed purple line. (**c**) Chemical structures of developed decapeptides derived from H3$_{4-13}$K9cr.
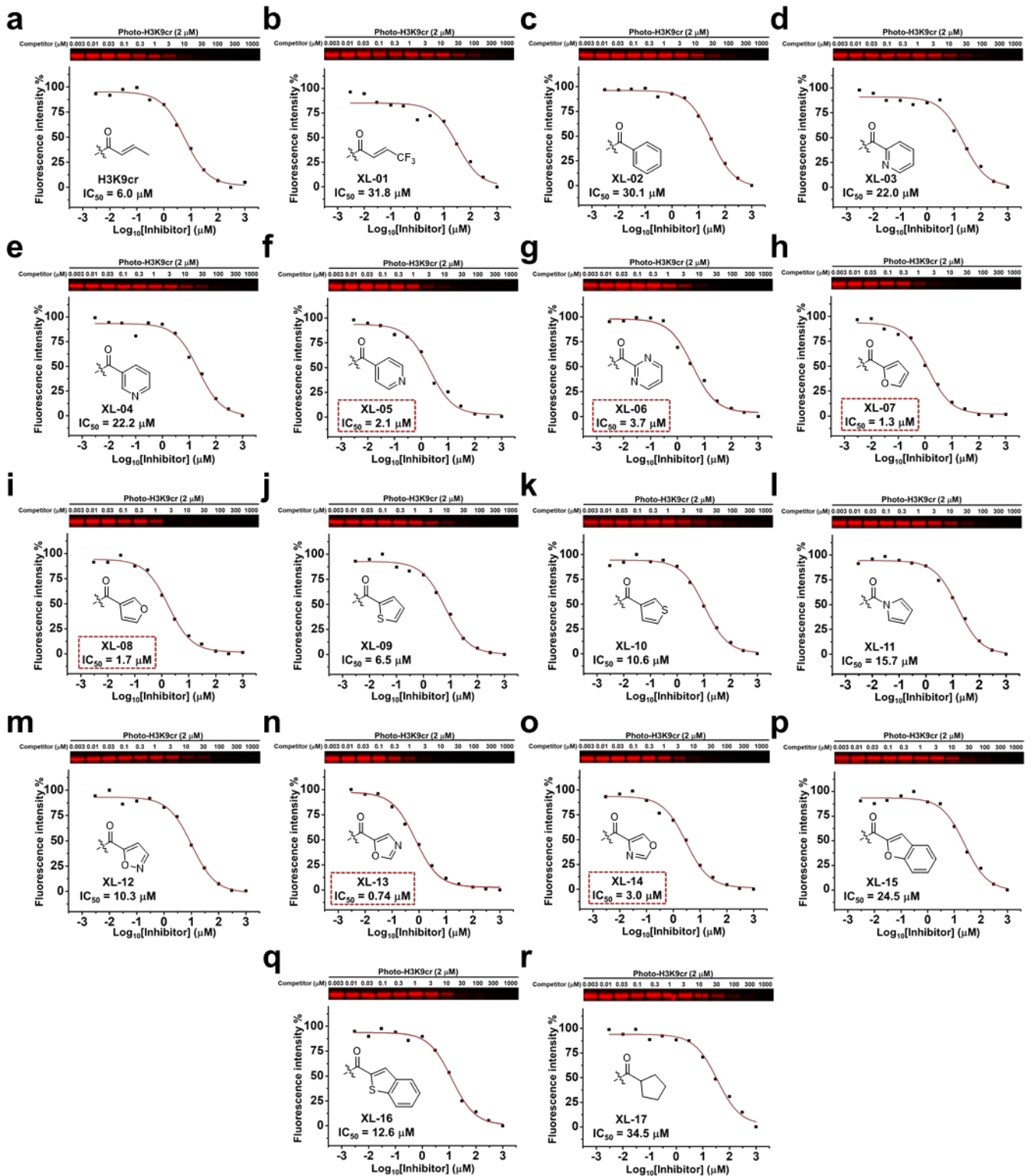
Supplementary Figure 2. Determination of the inhibitory effects of developed decapeptides against AF9 YEATS domain by competitive photo-cross-linking assay. The functional groups on the lysine side chain of each decapeptide was showed with the competition curve. Decapeptides with IC_{50} lower than that of the H3K9cr peptide against AF9 YEATS were circled by dashed red rectangle. For all the competitive photo-cross-linking assay, after UV irradiation, the photo-H3K9cr-labeled protein was conjugated to rhodamine-N_3 and visualized by in-gel fluorescence scanning. The fluorescence intensity of each band was quantified by ImageJ. All curves were normalized between 100% and 0% at the highest and lowest fluorescence intensities, respectively. Data are reported as mean of two independent experiments. Uncropped gels are provided in Supplementary Fig 12.

a

b
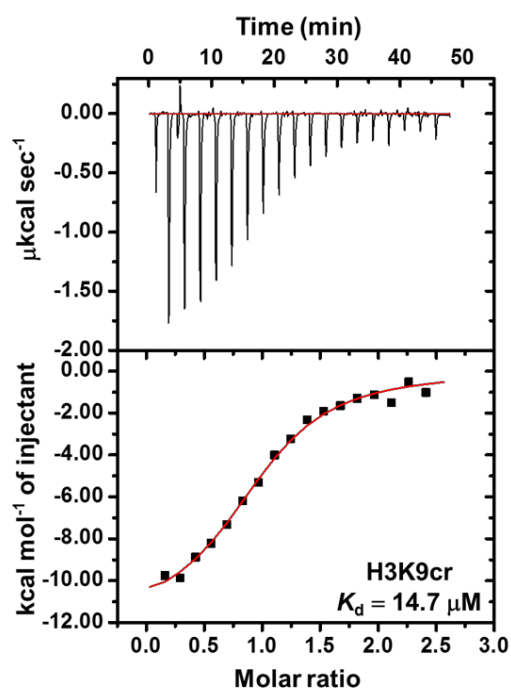
| Compound	K_d (µM)	ΔH (cal/mol)	ΔS (cal/mol/deg)
H3K9cr	14.7	-11920 ± 423	-17.8
XL-07	3.3	-12230 ± 110	-15.9
XL-13	1.0	-12290 ± 376	-13.8
XL-07i	0.33	-20080 ± 792	-37.7
XL-13a	0.13	-20390 ± 437	-36.9

Supplementary Figure 3. ITC measurements of the binding affinities between AF9 YEATS and selected oligopeptides. (**a**) ITC titration curve between H3K9cr peptide and AF9 YEATS. (**b**) Thermodynamic parameters of AF9 YEATS titrated with the selected oligopeptides. For the titration curves of XL-07, XL-13, XL-07i, and XL-13a, see Figure 2. For each of the ITC experiment of AF9 YEATS domain with the indicated peptides was repeated three times independently with similar results. Data are reported as mean ± s.d.
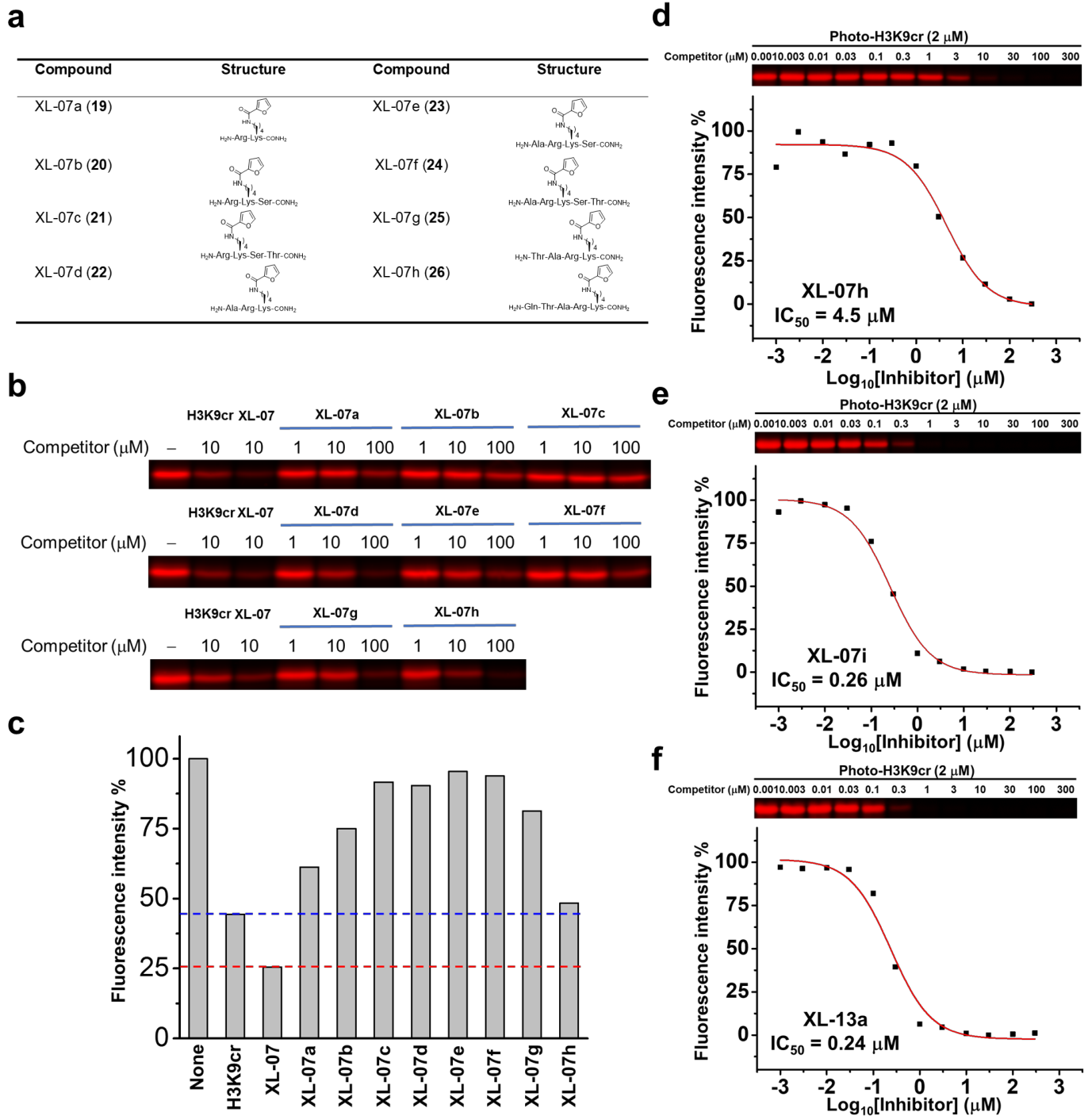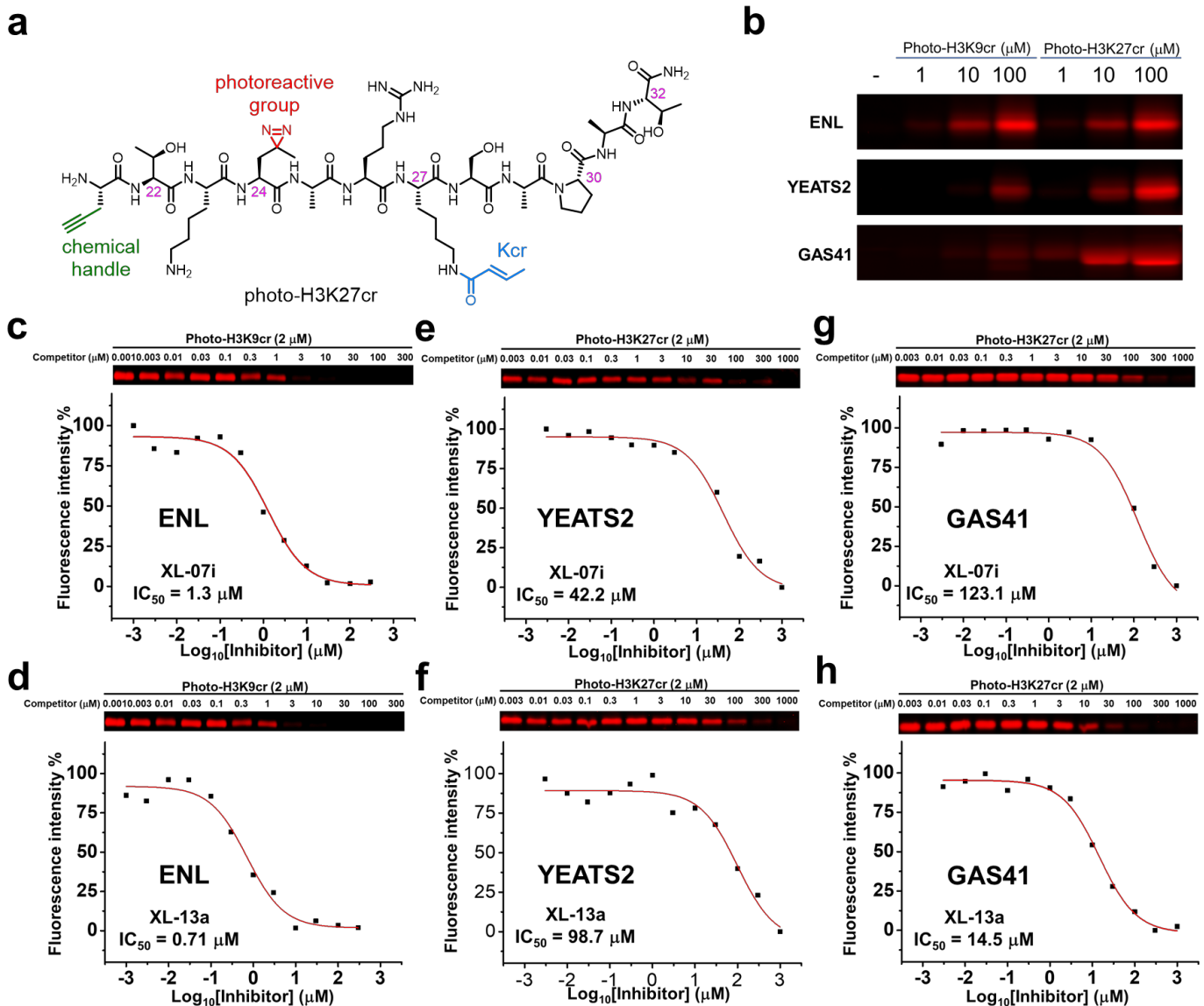
Supplementary Figure 4. Structure optimization for better inhibitory effects. (**a**) Chemical structures of oligopeptides XL-07a to XL-07h. (**b**) Three-spot competitive photo-cross-linking assay to screen the inhibitory effects of the oligopeptides against AF9 YEATS. Samples without competitor and using H3$_{4\text{-}13}$K9cr or XL-07 as competitors were prepared as controls. The experiment was performed once. (**c**) Histogram showing the inhibitory effects of oligopeptides XL-07a to XL-07h. Fluorescence intensity data were quantified from gels showed in (**b**). For each oligopeptide, the 10 μM spot data were used. Fluorescence intensity without competitor was normalized to 100%. Competition curves of (**d**) XL-07h, (**e**) XL-07i, and (**f**) XL-13a, respectively, against AF9 YEATS. For all the competitive photo-cross-linking assay, after UV irradiation, the photo-H3K9cr-labeled protein was conjugated to rhodamine-N$_3$ and visualized by in-gel fluorescence scanning. The fluorescence intensity of each band was quantified by ImageJ. All curves were normalized between 100% and 0% at the highest and lowest fluorescence intensities, respectively. Data are reported as mean of two independent experiments. Uncropped gels are provided in Supplementary Fig 12.
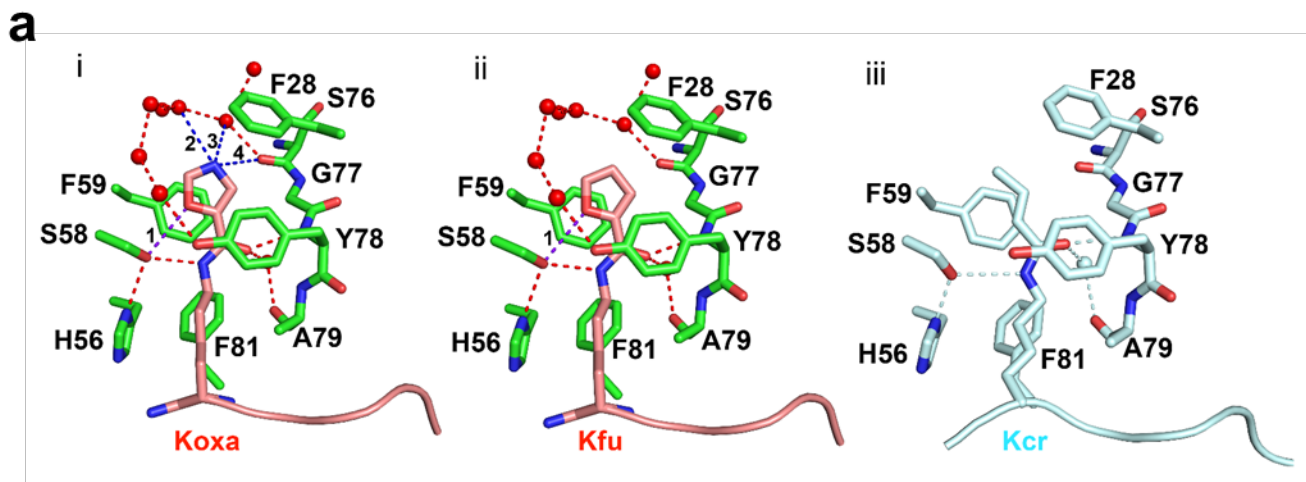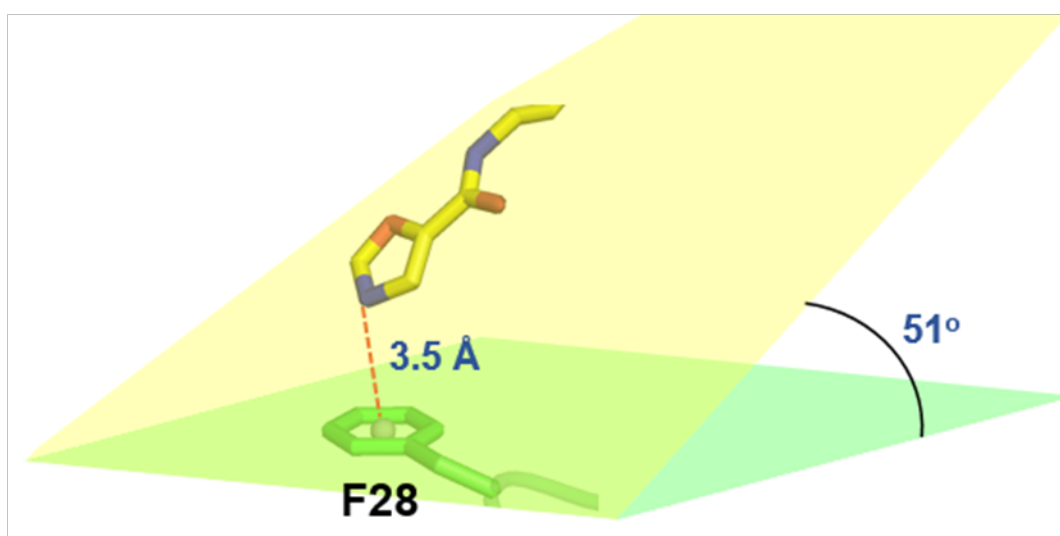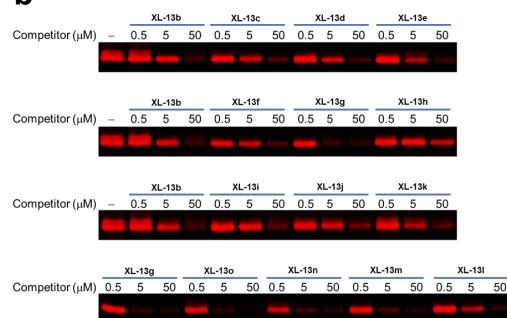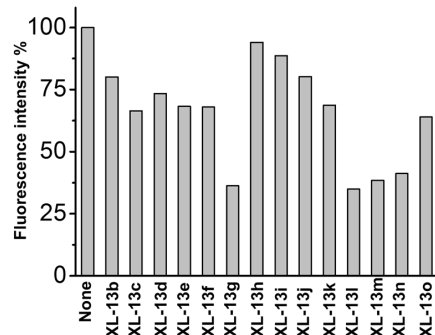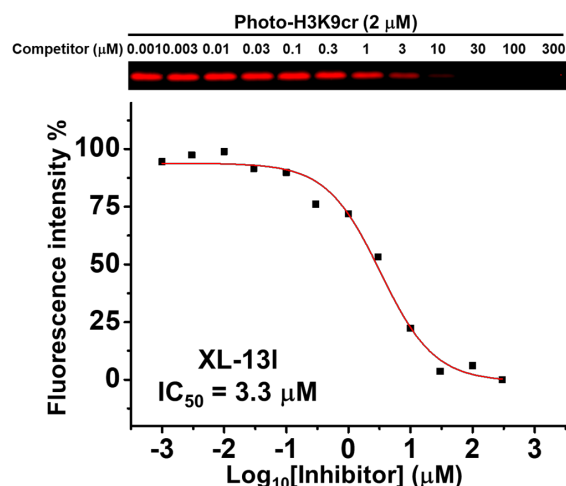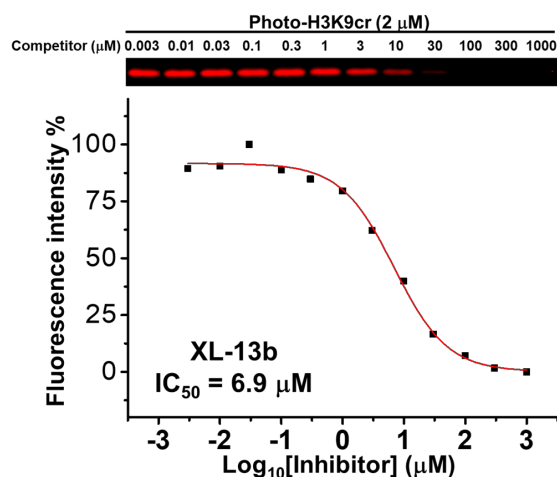
Supplementary Figure 5. *In silico* model of AF9-XL-13a. (a) Comparison of hydrogen bonding networks in the model of AF9 YEATS-XL-13a (i) and crystal structures of AF9 YEATS-XL-07i (ii) and AF9 YEATS-H3K9cr (iii). Red and cyan dashes, hydrogen bonds; red and cyan balls, water molecules; purple and blue dashes and numbers (1 to 4), additional hydrogen bonds compared with that of H3K9cr-binding. Kfu: 2-furancarbonyl lysine. Koxa: 5-oxazolecarbonyl lysine. **(b)** The oxazole nitrogen of XL-13a forms a lone pair-π interaction with F28 of AF9 YEATS. The distance from the nitrogen to the phenyl ring centroid of F28 is 3.5 Å; and the dihedral angle between the planes defined by the oxazole ring and F28 phenyl ring is 51°, indicating a moderate lone pair-π interaction between them. The oxazole ring of XL-13a and phenyl ring of F28 are placed in the yellow and green planes, respectively. Grey ball: centroid of F28 phenyl ring.
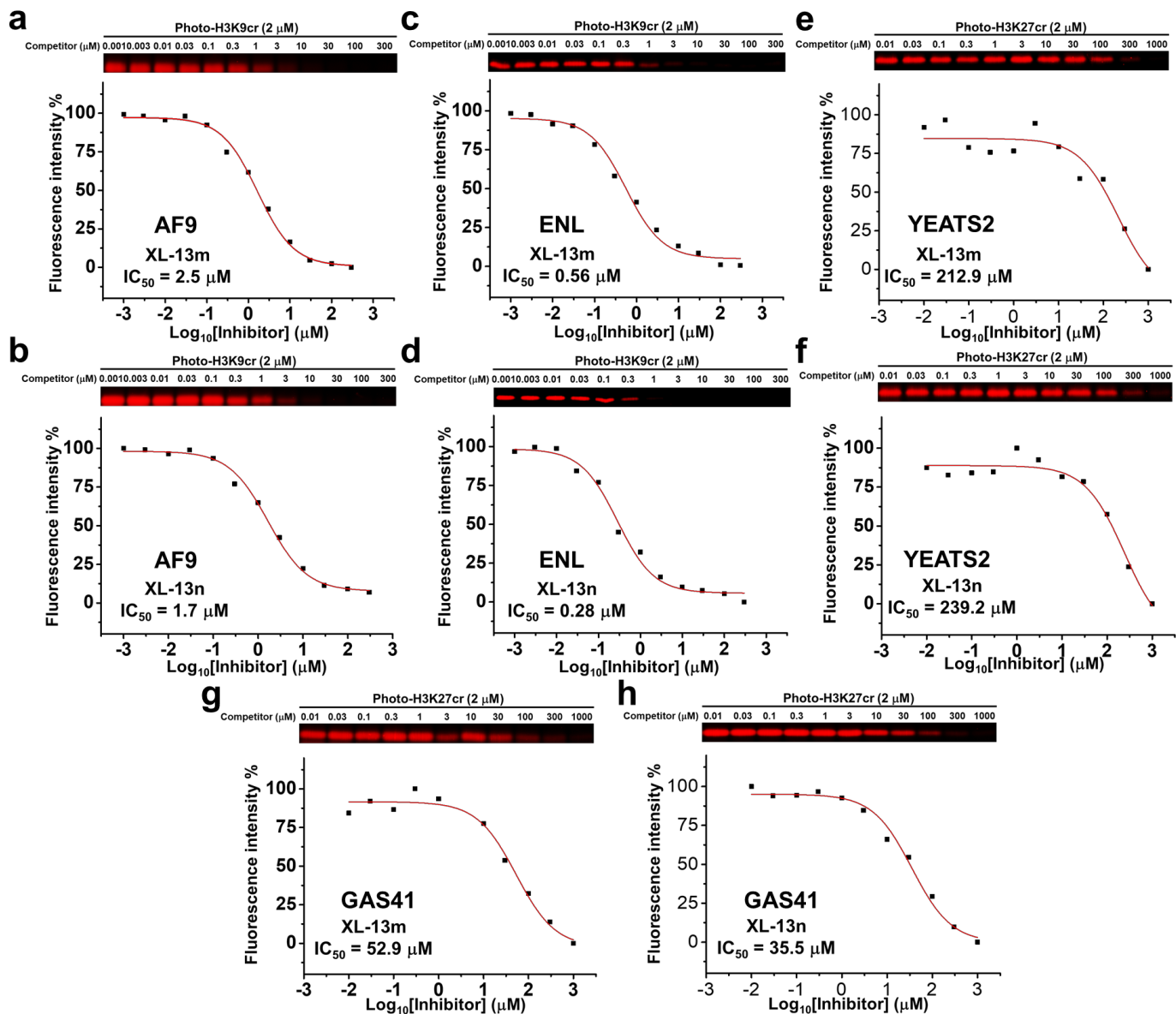
Supplementary Figure 6. Selectivity of XL-07i and XL-13a on different YEATS domains. (**a**) Chemical structure of photo-H3K27cr probe. Photo-H3K27cr was derived from H3 peptide with Lys 27 crotonylated. The design was guided by the reported crystal structure of YEATS2 YEATS domain in complex with H3K27cr peptide (D. Zhao *et al.*, *Cell Res.*, **2016**, 26, 629–632). (**b**) Comparison of the labeling efficiency of photo-H3K9cr and photo-H3K27cr toward different YEATS domains. For ENL YEATS, both probes resulted in similar labeling efficiency; while for YEATS2 and GAS41, photo-H3K27cr led to significantly higher labeling efficiency than photo-H3K9cr. The experiment was performed once. In the following photo-cross-linking experiments, therefore, photo-H3K9cr was used for ENL, photo-H3K27cr was used for YEATS2 and GAS41. (**c-g**) Competition curves of XL-07i and XL-13a against YEATS domains of ENL, YEATS2, and GAS41. For all the competitive photo-cross-linking assay, after UV irradiation, the photo-H3K9/27cr-labeled protein was conjugated to rhodamine-N_3 and visualized by in-gel fluorescence scanning. The fluorescence intensity of each band was quantified by ImageJ. All curves were normalized between 100% and 0% at the highest and lowest fluorescence intensities, respectively. Data are reported as mean of two independent experiments. Uncropped gels are provided in Supplementary Fig 12.

Supplementary Figure 7. Development of ENL YEATS-selective inhibitors (**a**) Chemical structures of oligopeptide XL-13b to XL-13o. (**b**) Three-spot competitive photo-cross-linking assay to screen the inhibitory effects of the oligopeptides against ENL YEATS. Sample without competitor was prepared as controls. The experiment was performed once. (**c**) Histogram showing the inhibitory effects of oligopeptides XL-13b to XL-13o. Fluorescence intensity data were quantified from gels showed in (**b**). For each oligopeptide, the 5 μM spot data were used. Fluorescence intensity without competitor was normalized to 100%. Competition curves of (**d**) XL-13l and (**e**) XL-13b, respectively, against ENL YEATS. For all the competitive photo-cross-linking assay, after UV irradiation, the photo-H3K9cr-labeled protein was conjugated to rhodamine-N_3 and visualized by in-gel fluorescence scanning. The fluorescence intensity of each band was quantified by ImageJ. All curves were normalized between 100% and 0% at the highest and lowest fluorescence intensities, respectively. Data are reported as mean of two independent experiments. Uncropped gels are provided in Supplementary Fig 12.

Supplementary Figure 8. Selectivity of XL-13m and XL-13n on different YEATS domains. (a-h) Competition curves of XL-13m and XL-13n against YEATS domains of AF9, ENL, YEATS2, and GAS41. For all the competitive photo-cross-linking assay, after UV irradiation, the photo-H3K9/27cr-labeled protein was conjugated to rhodamine-N_3 and visualized by in-gel fluorescence scanning. The fluorescence intensity of each band was quantified by ImageJ. All curves were normalized between 100% and 0% at the highest and lowest fluorescence intensities, respectively. Data are reported as mean of two independent experiments. Uncropped gels are provided in Supplementary Fig 12.
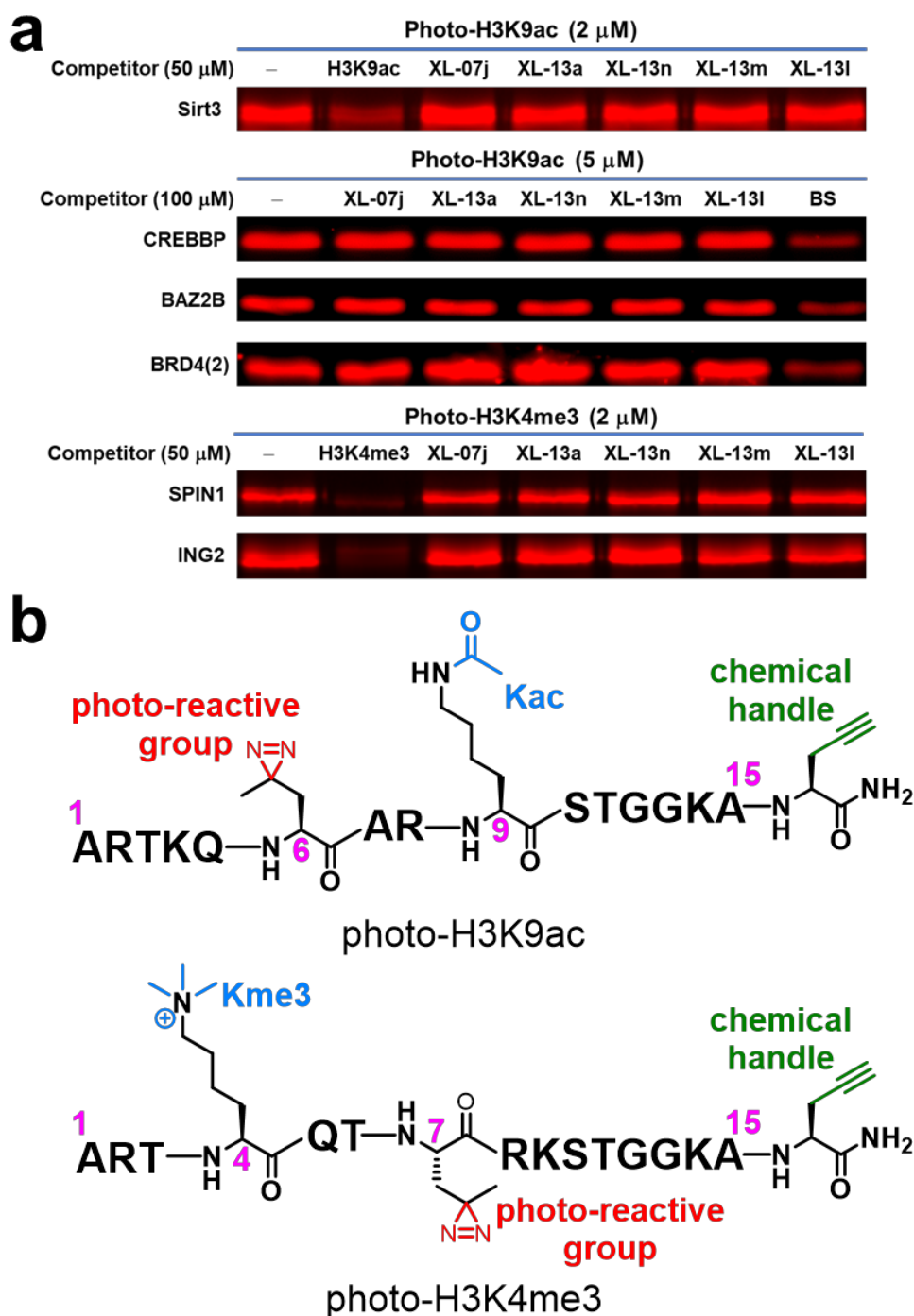
Supplementary Figure 9. The developed YEATS inhibitors are inactive toward other epigenetic regulators. (**a**) One-spot competitive photo-cross-linking assay to screen the inhibitory effects of the developed peptides against Kac 'eraser' Sirt3, Kac 'readers' bromodomains of CREBBP, BAZ2B, BRD4, and methylation 'reader' SPIN1 and ING2. Sample without competitor, or with known binding partners were prepared as controls. Experiment was performed once. H3K9ac: histone H3 peptide with Lys 9 acetylated. BS: bromosporine, a pan-BrD inhibitor. H3K4me3: histone H3 peptide with Lys 4 trimethylated. For all the competitive photo-cross-linking assay, after UV irradiation, the photo-H3K9ac/H3K4me3-labeled protein was conjugated to rhodamine-N_3 and visualized by in-gel fluorescence scanning. (**b**) Chemical structures of photo-H3K9ac and photo-H3K4me3 (T. Yang *et al.*, *Chem. Sci.*, **2015**, 6, 1011-1017). Uncropped gels are provided in Supplementary Fig 12.
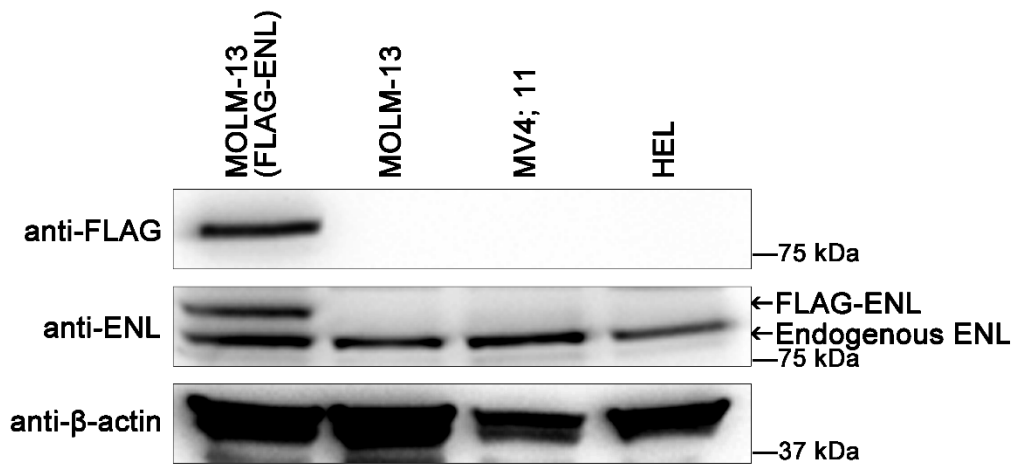
Supplementary Figure 10. Immunoblotting showing the ENL protein level in different leukemia cell lines. Note that the Flag-ENL level in MOLM-13 cells is equivalent to that of the endogenous one. Experiment was performed once. Uncropped gels are provided in Supplementary Fig 12.
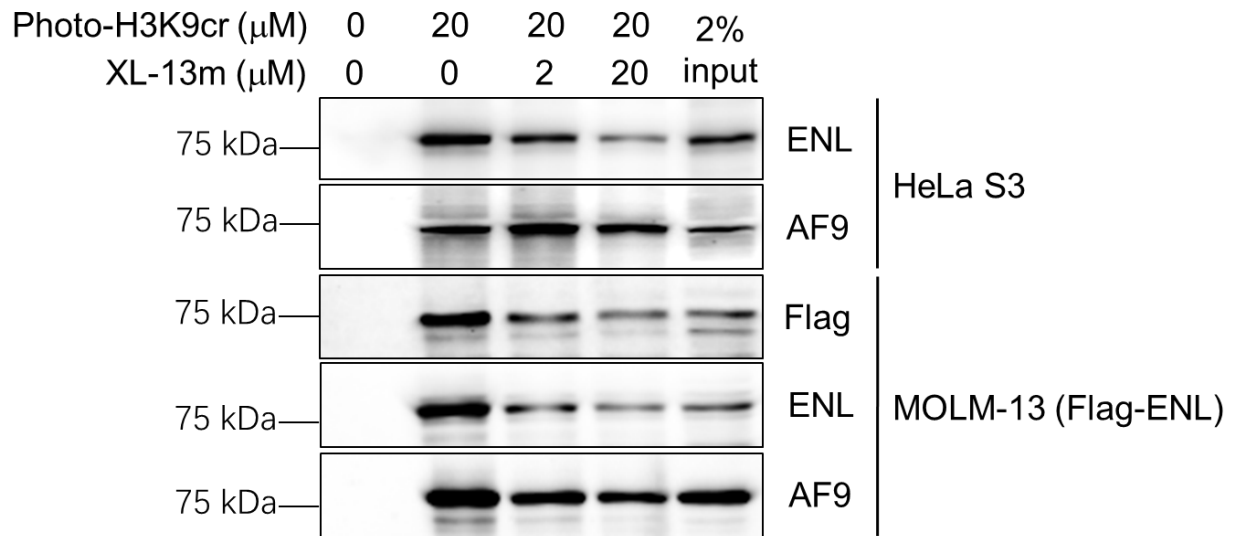
Supplementary Figure 11. Competitive pull-down assay showing the effects of XL-13m on the enrichment of ENL and AF9. *In-vitro* photo-cross-linking pulldown in nuclear extracts (1 mg/mL) with photo-H3K9cr (20 μM) in the presence of increasing concentrations of XL-13m. Samples without adding photo-H3K9cr was prepared as negative control. After photo-cross-linking, the photo-H3K9cr-labled proteins were conjugated to biotin-N$_3$ and enriched by streptavidin. The eluted protein mixtures were analyzed by immunoblotting against indicated antibodies. The experiment was performed once for each of the cell lines. Uncropped gels are provided in Supplementary Fig 12.

Uncropped gels and blots

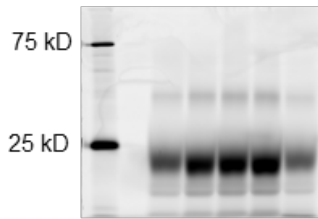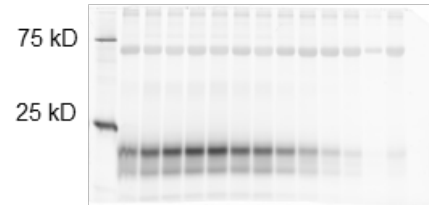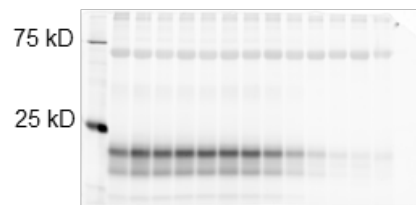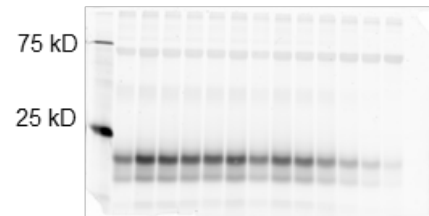Fig. 1d In-gel fluorescence labeling of photo-H3K9cr to AF9 YEATS
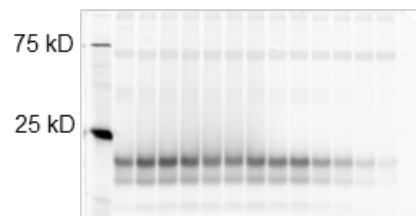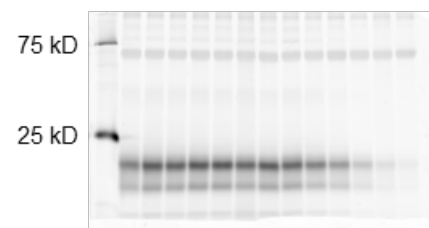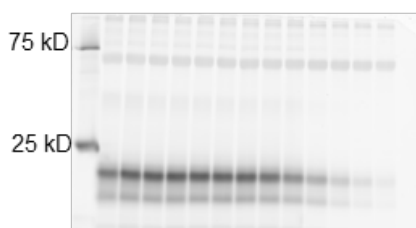

Fig. 2a, Supplementary Fig. 2a In-gel fluorescence AF9 YEATS competition by H3K9cr, two repeats

Supplementary Fig. 2b In-gel fluorescence AF9 YEATS competition by XL-01, two repeats

Supplementary Fig. 2c In-gel fluorescence AF9 YEATS competition by XL-02, two repeats

Supplementary Fig. 2d In-gel fluorescence AF9 YEATS competition by XL-03, two repeats
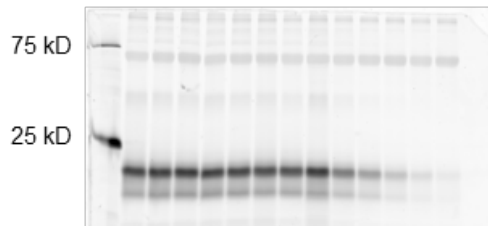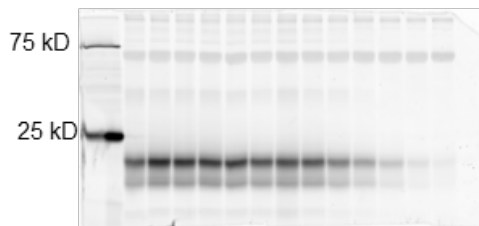

Supplementary Fig. 2e In-gel fluorescence AF9 YEATS competition by XL-04, two repeats

Supplementary Fig. 2f In-gel fluorescence AF9 YEATS competition by XL-05, two repeats

Uncropped gels and blots (continued)

Supplementary Fig. 2g In-gel fluorescence AF9 YEATS competition by XL-06, two repeats
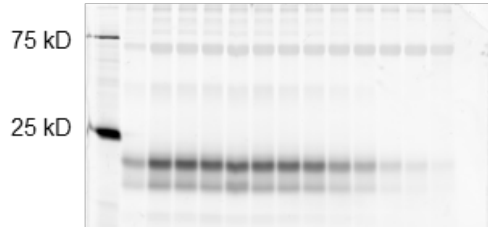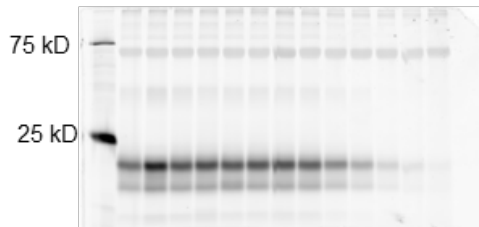

Fig 2a, 2d, Supplementary Fig. 2h In-gel fluorescence AF9 YEATS competition by XL-07, two repeats

Supplementary Fig. 2i In-gel fluorescence AF9 YEATS competition by XL-08, two repeats

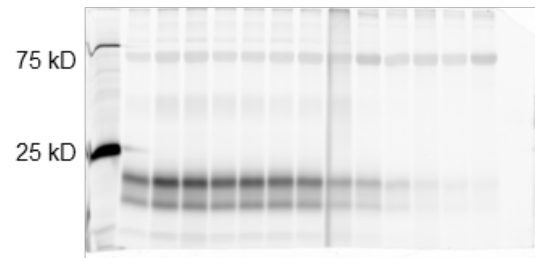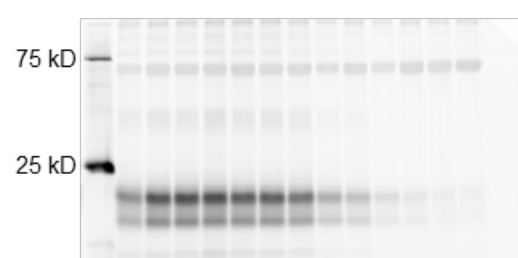
Supplementary Fig. 2j In-gel fluorescence AF9 YEATS competition by XL-09, two repeats

Supplementary Fig. 2k In-gel fluorescence AF9 YEATS competition by XL-10, two repeats

Supplementary Fig. 2l In-gel fluorescence AF9 YEATS competition by XL-11, two repeats

Supplementary Fig. 2m In-gel fluorescence AF9 YEATS competition by XL-12, two repeats
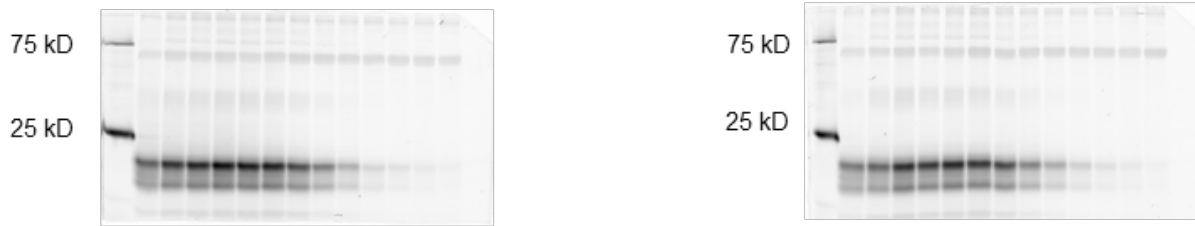
Uncropped gels and blots (continued)

Fig. 2a, 2d, Supplementary Fig. 2n In-gel fluorescence AF9 YEATS competition by XL-13, two repeats

Supplementary Fig. 2o In-gel fluorescence AF9 YEATS competition by XL-14, two repeats
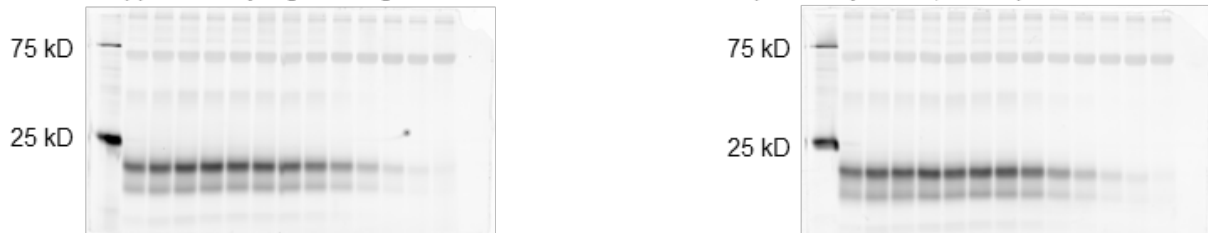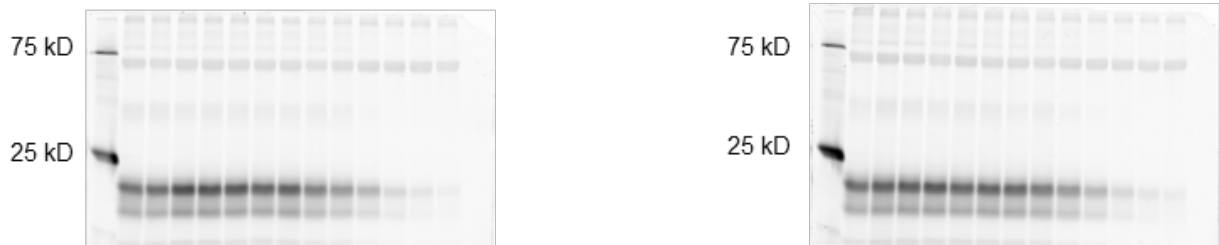

Supplementary Fig. 2p In-gel fluorescence AF9 YEATS competition by XL-15, two repeats

Supplementary Fig. 2q In-gel fluorescence AF9 YEATS competition by XL-16, two repeats

Fig 2a, Supplementary Fig. 2r In-gel fluorescence AF9 YEATS competition by XL-17, two repeats

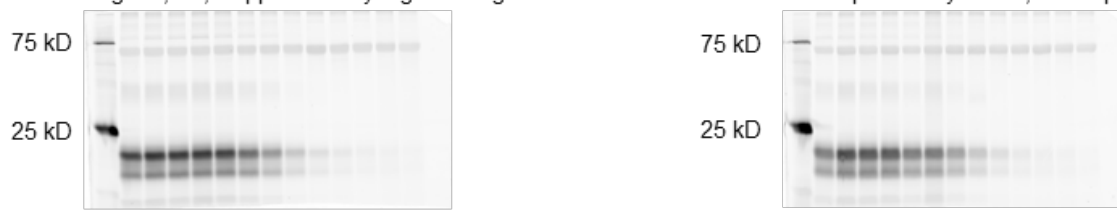Supplementary Fig. 4b In-gel fluorescence AF9 YEATS 3-spot competition screening by XL-07a to XL-07h

Supplementary Fig. 4d In-gel fluorescence AF9 YEATS competition by XL-07h, two repeats

Uncropped gels and blots (continued)

Fig. 2d, Supplementary Fig. 4e In-gel fluorescence AF9 YEATS competition by XL-07i, two repeats

Fig. 2d, 4a, Supplementary Fig. 4f In-gel fluorescence AF9 YEATS competition by XL-13a, two repeats

Supplementary Fig. 6b In-gel fluorescence labeling of photo-H3K9/27cr to ENL, YEATS2, GAS41 YEATS

Supplementary Fig. 6c In-gel fluorescence ENL YEATS competition by XL-07I, two repeats
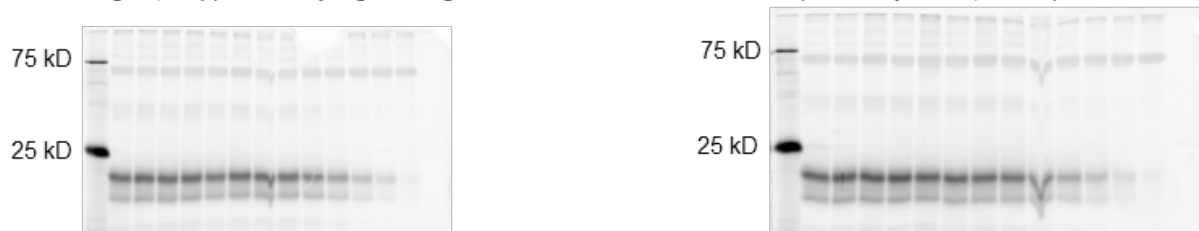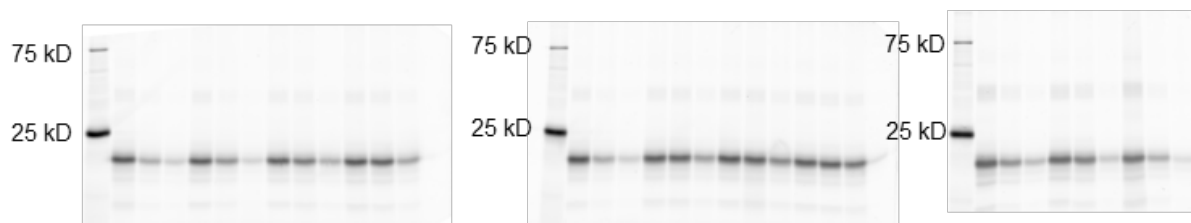

Fig. 4a, Supplementary Fig. 6d In-gel fluorescence ENL YEATS competition by XL-13a, two repeats

Supplementary Fig. 6e In-gel fluorescence YEATS2 YEATS competition by XL-07i, two repeats

Fig. 4a, Supplementary Fig. 6f In-gel fluorescence YEATS2 YEATS competition by XL-13a, two repeats

Uncropped gels and blots (continued)

Supplementary Fig. 6g In-gel fluorescence GAS41 YEATS competition by XL-07i, two repeats

Fig. 4a, Supplementary Fig. 6h In-gel fluorescence GAS41 YEATS competition by XL-13a, two repeats

Supplementary Fig. 7b In-gel fluorescence ENL YEATS 3-spot competition screening by XL-13b to XL-13l

Supplementary Fig. 7d In-gel fluorescence ENL YEATS competition by XL-13l, two repeats

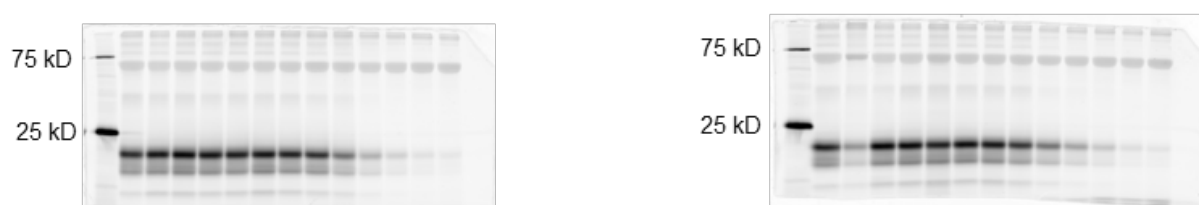Supplementary Fig. 7e In-gel fluorescence ENL YEATS competition by XL-13b, two repeats

Fig. 4c, Supplementary Fig. 8a In-gel fluorescence AF9 YEATS competition by XL-13m, two repeats
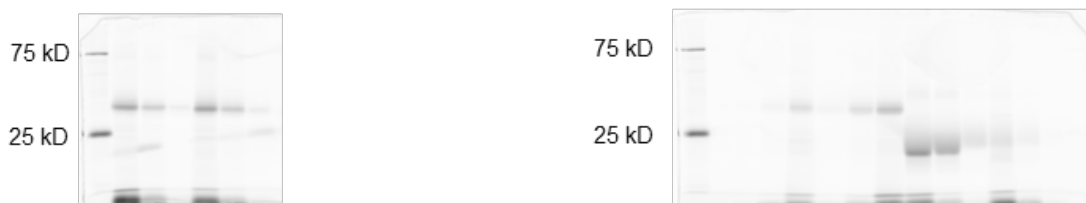
Uncropped gels and blots (continued)

Fig. 4c, Supplementary Fig. 8b In-gel fluorescence AF9 YEATS competition by XL-13n, two repeats

Fig. 4c, Supplementary Fig. 8c In-gel fluorescence ENL YEATS competition by XL-13m, two repeats
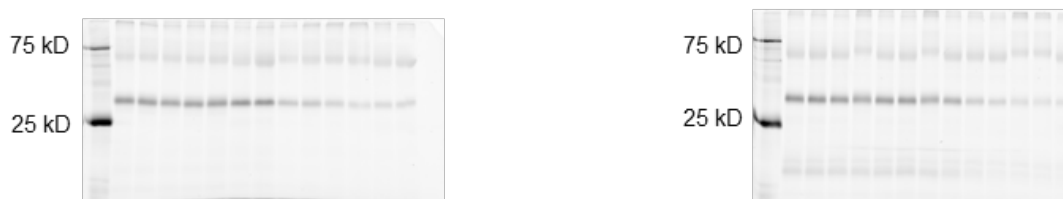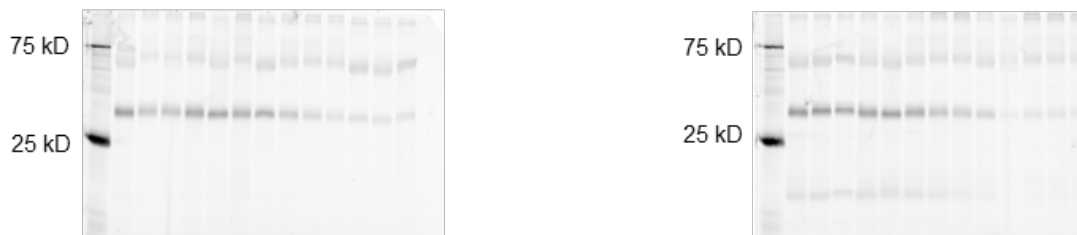

Fig. 4c, Supplementary Fig. 8d In-gel fluorescence ENL YEATS competition by XL-13n, two repeats

Supplementary Fig. 8e In-gel fluorescence YEATS2 YEATS competition by XL-13m, two repeats

Supplementary Fig. 8f In-gel fluorescence YEATS2 YEATS competition by XL-13n, two repeats

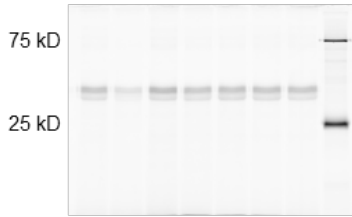Supplementary Fig. 8g In-gel fluorescence GAS41 YEATS competition by XL-13m, two repeats

Supplementary Fig. 8h In-gel fluorescence GAS41 YEATS competition by XL-13n, two repeats
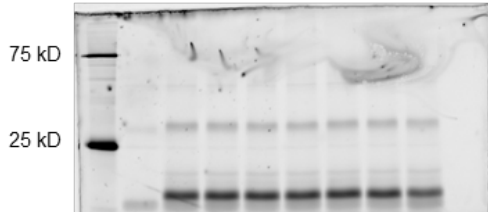
Uncropped gels and blots (continued)

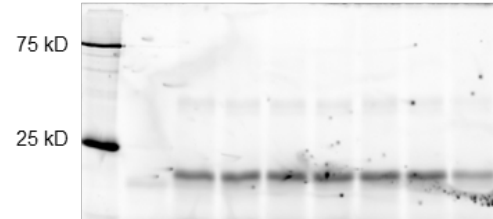Supplementary Fig. 9a In-gel fluorescence Sirt3

75 kD
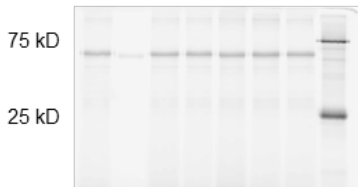
25 kD

Supplementary Fig. 9a, In-gel fluorescence CREBBP

75 kD

25 kD

Supplementary Fig. 9a, In-gel fluorescence BAZ2B

75 kD

25 kD

Supplementary Fig. 9a, In-gel fluorescence BRD4(2)

75 kD

25 kD

Supplementary Fig. 9a, In-gel fluorescence SPIN1

75 kD

25 kD

Supplementary Fig. 9a, In-gel fluorescence ING2

75 kD

25 kD
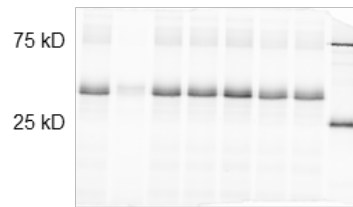
Fig. 5a, anti-ENL, three repeats

150 kD
75 kD
50 kD
37 kD
25 kD

150 kD
75 kD
50 kD
37 kD
25 kD

150 kD
75 kD
50 kD
37 kD
25 kD
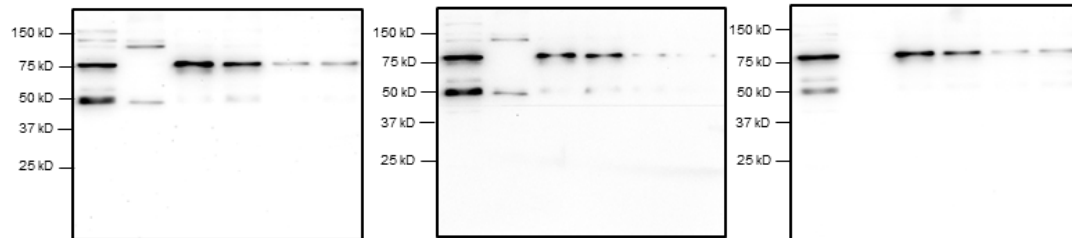
Fig. 5a, anti-AF9, three repeats

150 kD
75 kD
50 kD
37 kD
25 kD

150 kD
75 kD
50 kD
37 kD
25 kD

150 kD
75 kD
50 kD
37 kD
25 kD
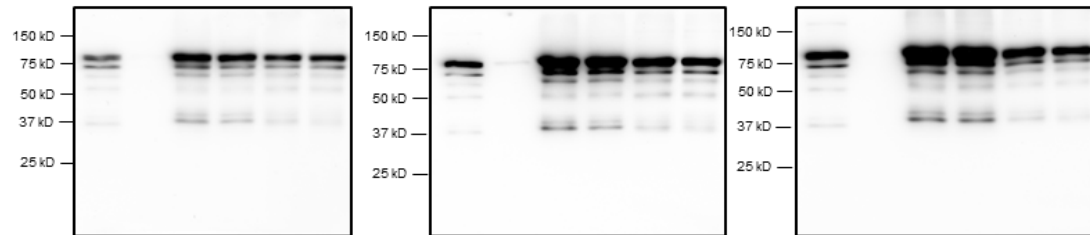
Supplementary Fig. 11, MOLM13 (FLAG-ENL), anti-FLAG (left), anti-ENL (middle), anti-AF9 (right)

150 kD
75 kD
50 kD
37 kD
25 kD

150 kD
75 kD
50 kD
37 kD
25 kD

150 kD
75 kD
50 kD
37 kD
25 kD
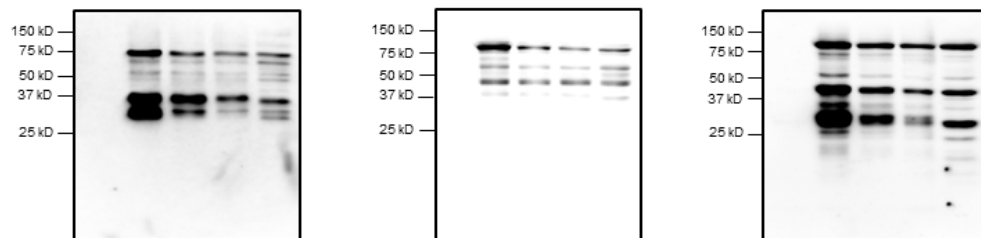
Supplementary Fig. 11, HeLa S3, anti-ENL (LEFT), anti-AF9 (right)

150 kD
75 kD
50 kD
37 kD
25 kD

150 kD
75 kD
50 kD
37 kD
25 kD

Uncropped gels and blots (continued)

Figure 5c_MOLM13_anti-FLAG

←150 kD
←75 kD
←50 kD
←37 kD

Figure 5c_MOLM13_anti-γ-actin

←75 kD
←50 kD
←37 kD
←25 kD

Figure 5c_MV4;11_anti-γ-actin

←75 kD
←50 kD
←37 kD

Figure 5d_MOLM13_anti-AF9

←150 kD
←75 kD
←50 kD
←37 kD

Figure 5d_MV4;11_anti-AF9

←100 kD
←75 kD
←50 kD
←37 kD

Figure 5d_HEL_anti-AF9

←150 kD
←75 kD
←50 kD

Supplementary Figure 10_anti-FLAG

←150 kD
←75 kD
←50 kD

Supplementary Figure 10_anti-ENL

←150 kD
←50 kD
←75 kD

Figure 5c_MOLM13_anti-ENL

←150 kD
←75 kD
←50 kD
←37 kD

Figure 5c_MV4;11_anti-ENL

←150 kD
←75 kD
←50 kD
←37 kD

Figure 5c_HEL_anti-ENL

←100 kD
←75 kD
←50 kD

Figure 5c_HEL_anti-γ-actin

←50 kD
←37 kD

Figure 5d_MOLM13_anti-γ-actin

←75 kD
←50 kD
←37 kD

Figure 5d_MV4;11_anti-γ-actin

←75 kD
←50 kD
←37 kD

Figure 5d_HEL_anti-γ-actin

←75 kD
←50 kD

Supplementary Figure 10_anti-actin

←50 kD
←37 kD

Supplementary Figure 12. Uncropped gels and blots.